AQUA
Water Infrastructure, Ecosystems and Society

IWA PUBLISHING

 AQUA — Water Infrastructure, Ecosystems and Society Vol 72 No 6, 996 doi: 10.2166/aqua.2023.020

Optimization of batch study parameters for the adsorption of lead(II) ions onto spent tea grains

Surendra Singh Chauhan* and Prabhat Kumar Singh Dikshit
Department of Civil Engineering, IIT-BHU, Varanasi, Uttar Pradesh, India
*Corresponding author. E-mail: surender.rs.civ17@itbhu.ac.in

ABSTRACT

The present study aims to investigate the use of response surface methodology (RSM) modelling and experimental investigation for the optimization of lead(II) adsorption onto spent tea grains (STG). Independent process variables were optimized and found to be in the range of 38.75 mg/l (initial concentration), 5.20655 (pH), 119.32 rpm (stirring speed), and 3.25 g/l (STG dose) for a contact time of 135.05 min. The optimum adsorption capacity was found to be 8.9087 mg/g through RSM modelling with a maximum of 18.146 mg/g. The batch study was performed by varying different parameters: pH (2.0–7.0), initial concentration (5–50 mg/l), dose (0.1–1 g/100 ml), contact time (15–180 min), and stirring speed (30–200 rpm). The characterization STG was done by proximate and ultimate analysis, FTIR spectroscopy, XRD analysis, thermogravimetric analysis (TGA), and SEM-EDX. By fitting equilibrium data onto Langmuir isotherm model, the maximum adsorption capacity was found to be 24.272 mg/g. The optimum pH found for lead(II) adsorption onto STG was 5. At optimum conditions, the maximum removal efficiency of STG for lead(II) ions' adsorption is 94.33%. Based on the findings it is safe to conclude that the STG could be used as a potential adsorbent.

Key words: adsorption, agricultural waste, biosorbent, equilibrium isotherms, heavy metal, kinetics, spent tea grains

HIGHLIGHTS

- Agricultural waste converted into low-cost adsorbent.
- Removal efficiency and uptake capacity of lead(II) ions onto prepared adsorbent STG shows great potential.
- A detailed study was done using RSM modelling and various batch experimentation to find optimum values of parameters influencing adsorption.
- The present study can be used for developing sustainable treatment technology using STG as an alternative to activated carbon currently used.

INTRODUCTION

Contamination of surface and sub-surface water bodies due to rapid urbanization and industrialization is now a well-known phenomenon (Ahluwalia & Goyal 2005). Detection of toxic heavy metals in our natural environment has been a major problem for scientists worldwide (Singh & Singh 2012; Omar *et al.* 2022). These toxic heavy metals are affecting the health of our overall ecosystem and are a major health concern for human beings due to their non-biodegradability and bioaccumulation in different food chains (Yoshita *et al.* 2009). The awareness of today's toxicity driven limits is the major driver for our scientific community to find different methods to reduce toxic contaminates in the ecosystem. Discharge studies of surface and sub-surface water are also important for toxicity assessment (Omar 2015; Shekhar *et al.* 2021).

Lead, a highly toxic heavy metal, is one of the priority pollutants. Lead can be released into the environment by a vast number of industries, like battery manufacturing, electroplating, mining, pigments, paper, and pulp (Mondal 2010). WHO limits detection of a maximum of 0.005 mg/l in drinking water because at even very low concentrations it is causing various diseases and disorders. Therefore, the removal of lead from our ecosystem is currently one of the most important aims of our research community (Zuorro & Lavecchia 2010). Adsorption of toxic heavy metals onto low-cost locally available adsorbent is an area under development in the past decade (Bailey *et al.* 1999; Babel & Kurniawan 2003; Demirbas 2008). The various agricultural wastes are widely being investigated for their adsorption capabilities. These wastes are locally available in vast

amounts, and they are low-cost raw materials. Many researchers investigated the capability of such materials in removing different heavy metals from aqueous solutions like sugarcane, bagasse, leaves, rice husk (Marshall & Champagne 1995), sawdust (Shukla & Pai 2005), peanut hulls (Periasamy & Namasivayam 1995), peat moss (Simón *et al.* 2022), coconut shell (Sekar *et al.* 2004), and crop milling waste (Saeed *et al.* 2005).

A low-cost locally available adsorbent is one which can be found abundantly in nature or is a by-product or a waste from the nearby community (Lavecchia *et al.* 2010). Developing low-cost and more effective adsorbents for lead removal from biomass waste is a novel and promising area (Guclu *et al.* 2021; Ang *et al.* 2022). Tea, due to its well-known health benefits, is a widely consumed beverage worldwide. Spent Tea Grains (STG) are an agricultural waste compromising cellulose, hemicelluloses, condensed tannins, structural proteins, and lignin (Sahu *et al.* 2018). These above-mentioned constituents make tea waste a great candidate to replace activated carbon used in industry as an adsorbent in future as it contains various functional groups which help in metal scavenging, mainly carboxylate, phenolic hydroxyl, and oxyl groups (Hussain *et al.* 2018). The objective of the present study is to evaluate the efficiency of tea waste as an adsorbent for lead removal from an aqueous solution. A batch study experiment has been done to understand the effect of various parameters such as particle size, pH, initial concentration of metal, adsorbent dose and contact time.

MATERIALS AND METHODS

Chemical preparation

Lead(II) salt was used to prepare synthetic wastewater aqueous solutions. Double distilled water was used for preparation and dilution to the required concentration. The 1,000 mg/l stock solutions containing Pb (II) are obtained from Pb $(NO_3)_2$ salt of analytical grade. All glasswares used during the experimentation were properly washed and sterilised before and after the experimentation using chromic acid and then washed with distilled water.

Adsorbent preparation

The STG were obtained from different tea stalls on the campus of IIT BHU, Varanasi. The collected biomass waste is first dried in an oven at 80 °C for 12 h; however, instead of this collected biomass can be dried under sunlight for 2 days. Different constituents other than tea leaves/grains were then separated from it during preliminary screening. After this, the collected biomass waste was repeatedly boiled at above 100 °C and washed using distilled water for colour removal. After colour removal of the tea waste was completed, it was then oven dried by applying a temperature of 80 °C for 24 h. The sieving process was being applied to the prepared STG, particle range selected was in between 600 and 75 μm to be used for various batch experiments. The prepared adsorbent was stored in polyethylene bags at room temperature.

Characterization: instruments and techniques

The pH of the aqueous solutions used during different experiments was measured by using a digital pH meter. As pH is one of the most important parameters, its calibration was done with requisite precision. To identify different functional groups, present in STG, Fourier Transform Infrared Spectroscopy was investigated. Functional groups indicate adsorbent capability towards heavy metal scavenging, it also gives us an idea about the adsorption mechanism (Hammud *et al.* 2016). A spectra range of 600–4,000 cm^{-1} was selected to determine different functional groups present in the STW samples. SEM-EDS analysis was done to understand the morphological characteristics of the prepared adsorbent. SEM-EDS analysis was performed at an acceleration voltage of 5–15 kV and an EDAX detector using a microscope equipped with an energy dispersive analytical system. Elemental analysers were used for determining the elemental composition of the prepared adsorbent STG. Proximate analysis for determining fixed carbon, ash, moisture, and volatile matter was performed according to the ASTM D 2866-94, IS code 1350 (Part 1), and ASTM D 2867-95 methods. For investigating the structural properties of the adsorbent, X-ray diffraction (XRD) analysis was performed on the prepared adsorbent. XRD analysis is used to indicate crystal structural characteristics which give us an idea about its metal scavenging capabilities. Thermal degradation characteristics were investigated by thermogravimetric analysis (TGA). The TGA is very useful for determining the type of biomass composition, its moisture content and volatile matter composition. TGA is one of the effective techniques that are being used for pyrolysis optimization.

Determination of point-of-zero charge

The point-of-zero charge (pHzc) of the prepared adsorbent was investigated by the solid addition method. A series of 50 ml aqueous solutions of 0.1 M KNO_3 was transferred into a conical flask of capacity 100 ml. The pH for its determination was

adjusted from 2.0 to 12.0 by using dilute HNO_3 and dilute KOH. Then, 1.5 g of prepared adsorbent from STG was added to each conical flask. The conical flasks were then placed in a rotary shaker for 24 h at 150 rpm. After 24 h, the pH values of the supernatant are noted down. By analysing these values, we get the value of pHzc for the prepared adsorbent STG.

Experimental design with response surface methodology

Response surface methodology (RSM) is a powerful mathematical and statistical tool to analyze a wide variety of factors over a wide range to obtain responses, to identify the region of optimal response or to determine the near-optimal response by developing a designed experiment (Kavand *et al.* 2020). Central composite design under RSM was used for the optimization study. The advantage of using CCD using multilevel factorials in comparison to full factorial design is it will need fewer experiments to provide us with reliable information for statistical analyses. The ideal values of different process variables were calculated using the CCD model and then further validated by experiments (Sujatha & Sivarethinamohan 2021). The Design-Expert 13.0.5.0 (Stat-Ease) software was used for the regression and graphical analysis of the obtained data.

Firstly, some preliminary experiments were performed on lead(II) adsorption using STG as an adsorbent and the range and central points of all independent factors were determined. Different process variables and their ranges used in the model's computation were 5 and 50 mg/l for initial lead(II) ion concentration. The lower and upper limits of pH were 2 and 7, respectively. Similarly, the adsorbent dose was 1 and 10 g/l, respectively, the contact time was 30 and 180 min, respectively, stirring speed taken was 25 and 200 rpm, respectively. When this model is employed we will get 32 combinations of different test variables, namely A, B, C, D, E, AB, AC, AD, AE, BC, BD, BE, CD, CE, DE, A^2, B^2, C^2, D^2 and E^2.

Five independent parameters were designed with five coded values ($-\alpha$, -1, 0, $+1$, $+\alpha$). Thirty-two experiments were conducted with six replicates at the centre points. The ranges and actual levels are given in Table 1. In the optimization procedure, the response may be quadratic or linear (Shanmugaprakash *et al.* 2018). A quadratic model equation can be given as follows.

$$Y = \beta_0 + \sum_{i=1}^{k} \beta_i X_i \sum_{i=1}^{k} \beta_i X_i^2 + \sum_{i_{i<j}}^{k} \sum_{j}^{k} \beta_{ij} X_i X_j + \ldots . \quad (1)$$

where Y is the predicted response, β_i, β_j, and β_{ij} are the coefficients estimated from regression, X_i is the uncoded value of the ith variable, i is the linear coefficient, and k is the number of factors (Shanmugaprakash *et al.* 2018).

Validation of the model

Analysis of variance (ANOVA) tool is used for above developed CCD model with 95% confidence limits ($\alpha = 0.05$). Consideration of the model is only done after comparing the variance due to regression to that of the total variance (Gholamiyan *et al.* 2020). If they are different, then we will only consider the model developed to be validated. *F*-value and *p*-value will provide us with the significance of each factor. To provide the precise significance of the relationship between input variables, responses, and influential factors the ANOVA tool is utilized.

Batch adsorption experiments

To acquire kinetics and equilibrium data, different adsorption experiments were performed in a batch manner using an aqueous solution of Pb(II). For the determination of optimum values of different parameters which will affect adsorption

Table 1 | Factors and their corresponding values

	Levels				
Factors	**$-\alpha$**	**-1**	**0**	**$+1$**	**$+\alpha$**
pH	2.0	3.25	4.5	5.75	7.0
Contact time (min)	30	67.5	105	142.5	180
Initial metal ion conc. (mg/l)	5	16.25	27.5	38.75	50
Adsorbent dose (g/l)	1	3.25	5.5	7.75	10
Stirring speed (rpm)	25	68.75	112.5	156.25	200

efficiency, batch studies were performed. The pH values of the aqueous solutions were changed using weak acid, i.e. 1.0 M HNO_3 or weak base, i.e. 0.1 M NaOH solution whenever required during various experiments. Various factors considered during experiments were investigated including pH of the aqueous solutions (2.0–7.0), contact time (15–180 min), initial metal ion concentration from 5 to 50 mg/l, stirring speed (30–180 rpm), and adsorbent dose (1–5 g/l). The efficiency of adsorption is always dependent on the surface area available for adsorption. Therefore, the effect of particle size was investigated in the range of 75–150 μm, 150–300 μm, 300–600 μm, 600–900 μm, 900 μm–1.18 mm at room temperature, and maintaining other parameters as optimum during the experimentation.

Metal analysis

The aqueous solution was tested using atomic adsorption spectroscopy (AAS) which is based on Beer–Lambert's principle. A standard method was adopted to check for the concentrations of the lead(II). The rate of adsorption of the lead(II) ions and the rate of removal was calculated using the following equations, respectively:

$$Q_e = \frac{(C_o - C_e) * V}{1,000 * m} \tag{2}$$

$$Y(\%) = \frac{(C_o - C_e)}{C_o} * 100 \tag{3}$$

In the aforementioned Equation (2), Q_e is the amount of adsorbed lead(II) ions by the adsorbent STG in mg/g. The mass of adsorbent (i.e. STG) is represented by m in mg. The volume of the solution (ml) is indicated by V in Equation (3); Y (%) defines the removal efficiency of lead(II) ions by the adsorbent. C_o and C_e are, respectively, the initial and final concentrations of lead(II) in mg/l.

RESULTS AND DISCUSSION

Characterization

Proximate and ultimate analysis

Proximate analysis of STG will provide us with information about moisture, volatile matter, fixed carbon, and ash content, respectively. From the analysis of STG, we get the values fixed carbon content at 19.6%, there was a low ash content of 5.4%.

From the ultimate analysis of the STG, we found a reasonable amount of carbon content of approximately 47.541%. Detailed estimation of various parameters is mentioned in Table 2.

Point-of-zero charge

The pHzc of STG was determined as mentioned above. The pHpzc was calculated from the point where it crossed the $\Delta pH = 0$ and was found to be 7.57 ± 0.02 as shown in Figure 1.

Table 2 | Proximate and ultimate analysis of raw sample

Experiment	Content detected	Raw spent tea leaves: Content (%)
Proximate analysis	Moisture level	2.7
	Volatile matter	72.3
	Fixed carbon	19.6
	Ash content	5.4
Ultimate analysis	Carbon	47.541
	Hydrogen	6.533
	Nitrogen	4.100
	Sulphur	–
	Oxygen	[a]41.826

[a]*Note*: Oxygen content is deduced by deduction.

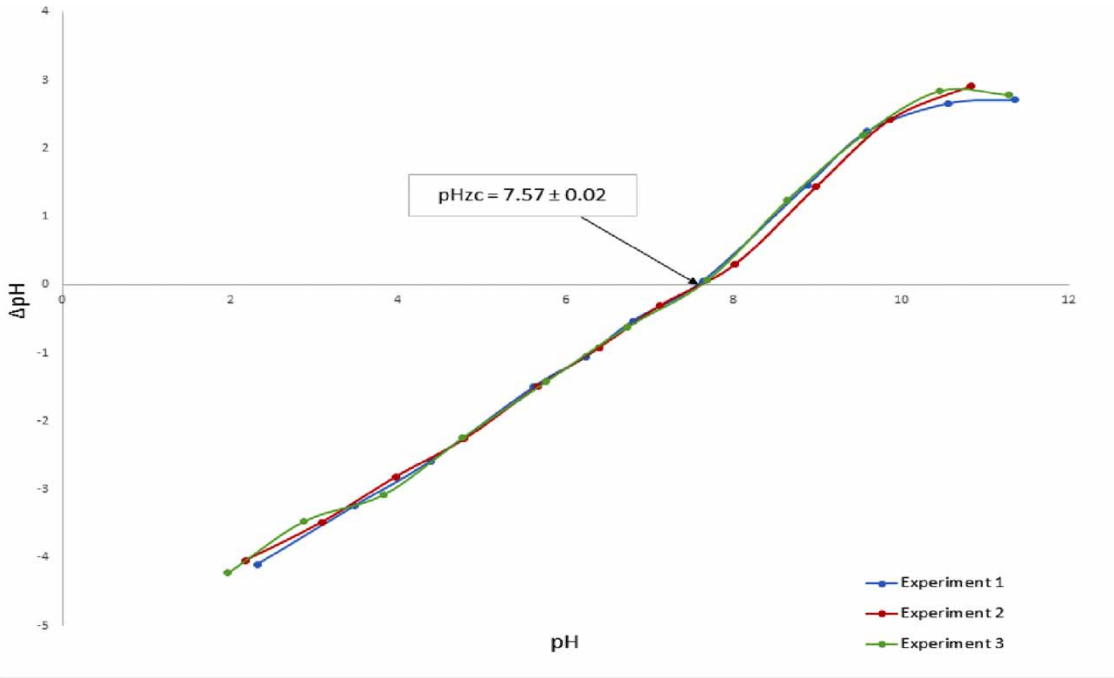

Figure 1 | pHzc of raw STG.

TGA of raw STG

To get the thermal stability and adsorbent decomposition profile we performed TGA. The thermogravimetric (TG) curve belonging to STG is presented in Figure 2. The degradation profile of STG took place in three main steps. At the initial stages when the temperature is less than 100 °C, an initial weight loss occurs that may be due to loss of moisture or to evaporation of the chemically strong and physically weak bound or to the release of lightweight volatiles from STG.

The initial weight loss in the first stage (20–200 °C) is around 8.29%. The second region of the STG transpires at around 250–415 °C. At a temperature of around 200 °C, a rapid devolatilization of the components starts and lasts until 410–415 °C, indicating the degradation of the fibre content of STG of hemicellulose, cellulose and attributed to the decomposition of holocellulose and partial decomposition of lignin. The contribution of weight loss during the second stage is about 51.48 wt.% and the maximum decomposition temperature was found to be in the region of 415 °C. In the second stage, the high weight loss may be due to the degradation of its main components by decarbonization, dehydration, and decarboxylation. The third stage of the STG is at 415–1,100 °C. The maximum decomposition temperature in this region is 1,100 °C. The weight loss in the third stage was due to the degradation of the lignin content of the STG. When the temperature reached 1,100 °C, the total weight loss of the STG is 93.49 wt.%.

Therefore, we can conclude from TGA that during our preparation of adsorbent at the initial stage when we applied a temperature of around 80 °C for 24 h weight loss occurred only due to loss of moisture, or loss of weak bonds, and there will be no chemical and structural modifications. Basically, during the preparation of STG, we are avoiding the degradation of lignin and cellulose functional groups responsible for the adsorption of lead(II) onto STG.

FTIR analysis of raw STG and lead ions-adsorbed STG

The FTIR spectroscopy technique was used to measure the various IR peaks of different functional groups of the STG. FTIR analysis was performed in the range of 500–4,000 cm^{-1} wave number. From Figure 2, we can see the complex IR spectra showing numerous different types of functional groups on the surface of STG. The difference between the IR peaks of different functional groups onto STG before and after lead(II) ions shows possible functional group involvement during the process of adsorption. Specific IR peaks due to unique energy bands before and after adsorption onto STG are provided as a useful tool to identify the involvement of certain functional groups during the adsorption process onto the surface of the STG.

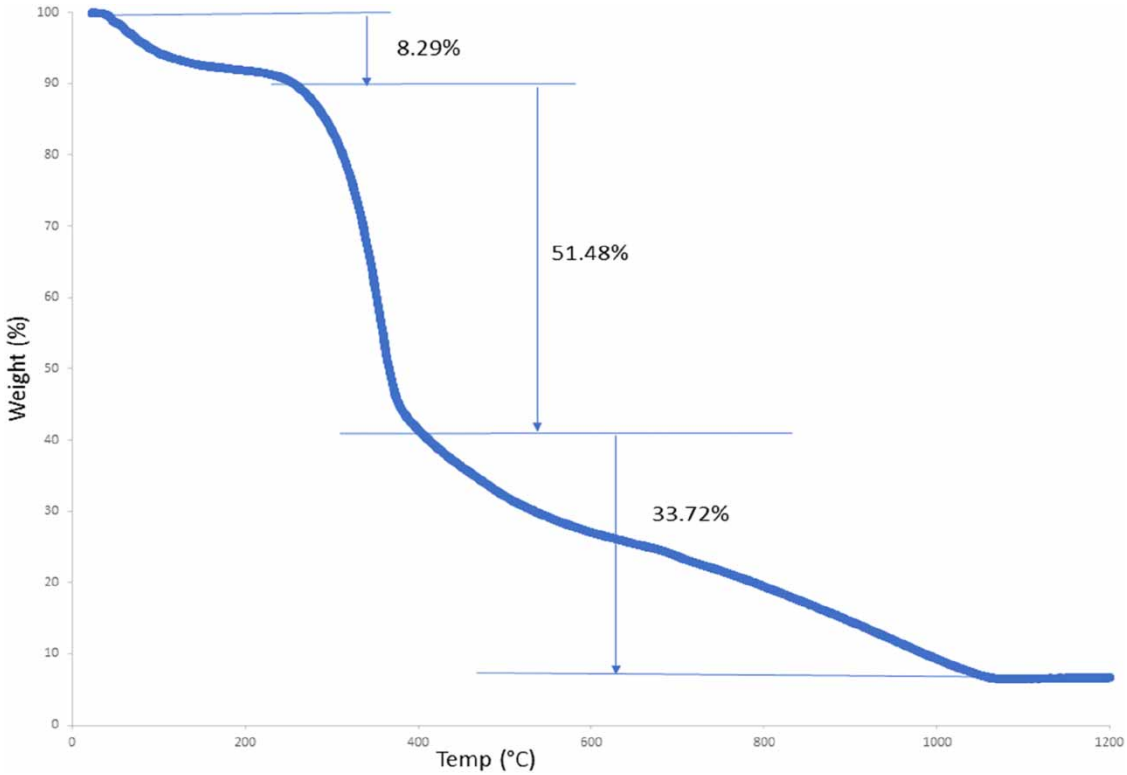

Figure 2 | TGA of raw STG.

At 3,351.2 cm^{-1} there is a presence of broad absorption bands, which signifies –OH stretching and confirms the presence of functional groups related to cellulose and lignin. The peaks appearing at about 3,016.6–2,859.5 cm^{-1} could be attributed to the aliphatic C–H groups, stretching in CH, CH_2, and CH_3 groups. The band observed at 1,641.96 cm^{-1} could be assigned to the asymmetric stretching vibrations of C = O stretching of the amide group and the peak appearing at around 1,475.51 cm^{-1} could be due to the aromatic compound group owing to the presence of N–H bending types of bonds of amide (II).

The other prominent bands observed at about 1,036.18 and 1,228.55 cm^{-1} are due to the C = O, NH_2 groups, and C–O stretching in alcohols. Some additional peaks were identified in the spectra of both samples. The peaks and bands shift can be easily observed in Figure 3. Henceforth, the shift in functional groups of –OH, C = O, $–NH_2$, –CH in STG before and after adsorption suggests the probable interactions of these functional groups with lead(II) ions, following the mechanism of hydrogen bonding, surface complex and electrostatic attraction.

XRD analysis of prepared adsorbent raw STG

The structural features will be analysed by XRD. XRD analysis on STG was performed to know the nature of its surface characteristics, i.e. amorphous or crystalline XRD profile of STG is shown in Figure 4. We can observe broad peaks in the XRD profile with the strongest reflection at 2θ around 22°, signifying the amorphous nature of STG which may be due to cellulose, hemicellulose, and lignin.

SEM-EDS analysis of raw STG and lead ions-adsorbed STG

SEM images will provide us with information about STG surface morphology. SEM images of the raw STG before and after dye biosorption of lead(II) ions are represented in Figure 5(a) and 5(b), showing varied pore size distribution. It clearly indicates the irregular, rough, and heterogeneous nature of STG. It also shows the presence of numerous cracks with voids onto the STG surface. However, after lead(II) ions adsorption (Figure 5(b)) the surface of STG is almost completely blanketed with lead(II) ions, affirming the occurrence of the adsorption mechanism of lead(II) ions onto the pores of STG.

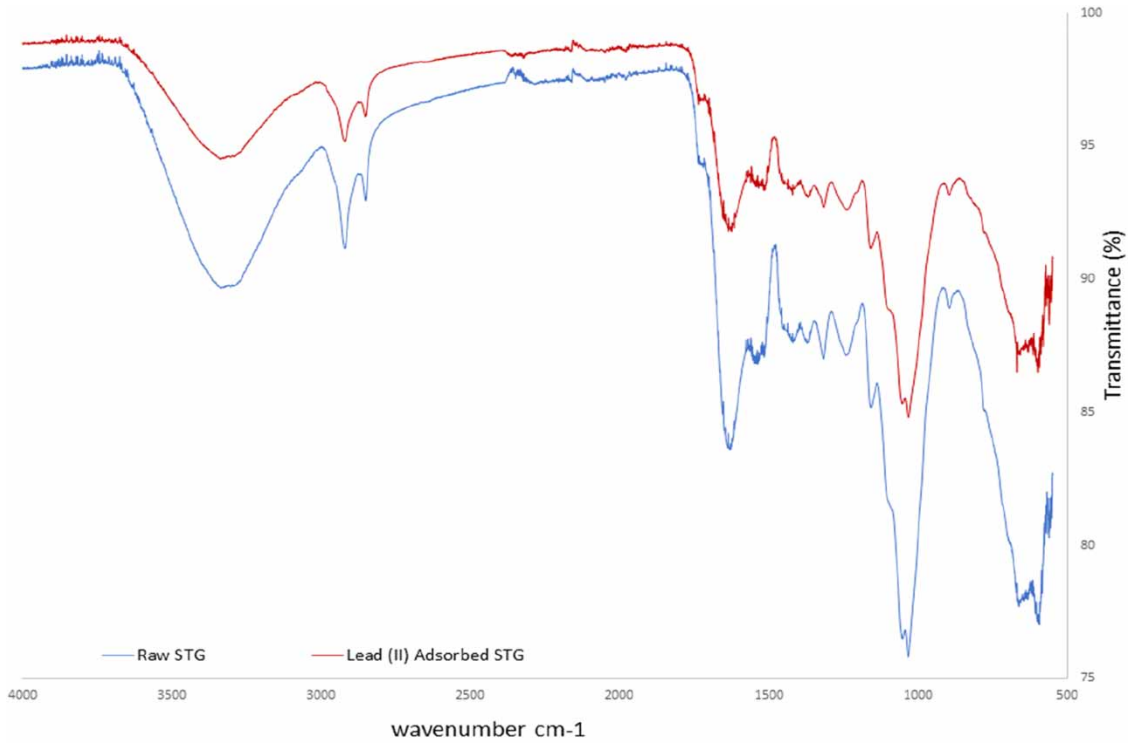

Figure 3 | FTIR analysis of raw STG and lead(II) ions-adsorbed STG.

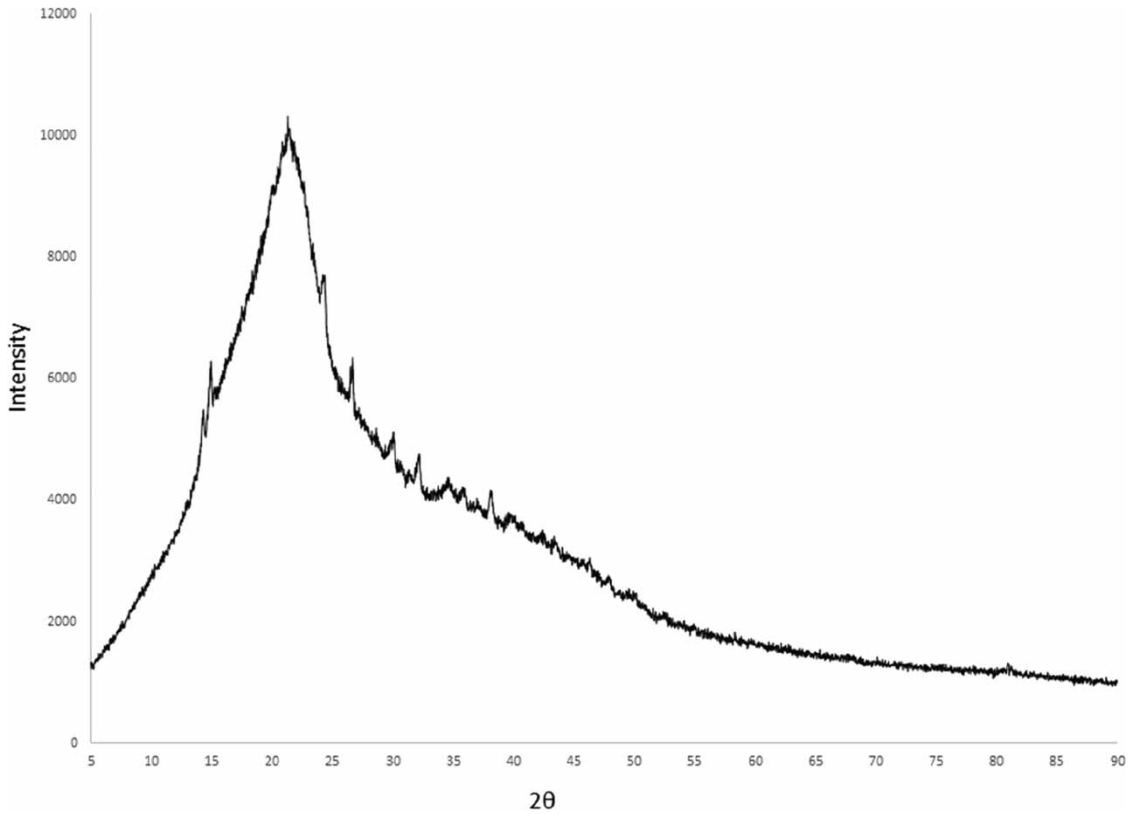

Figure 4 | XRD analysis of raw STG.

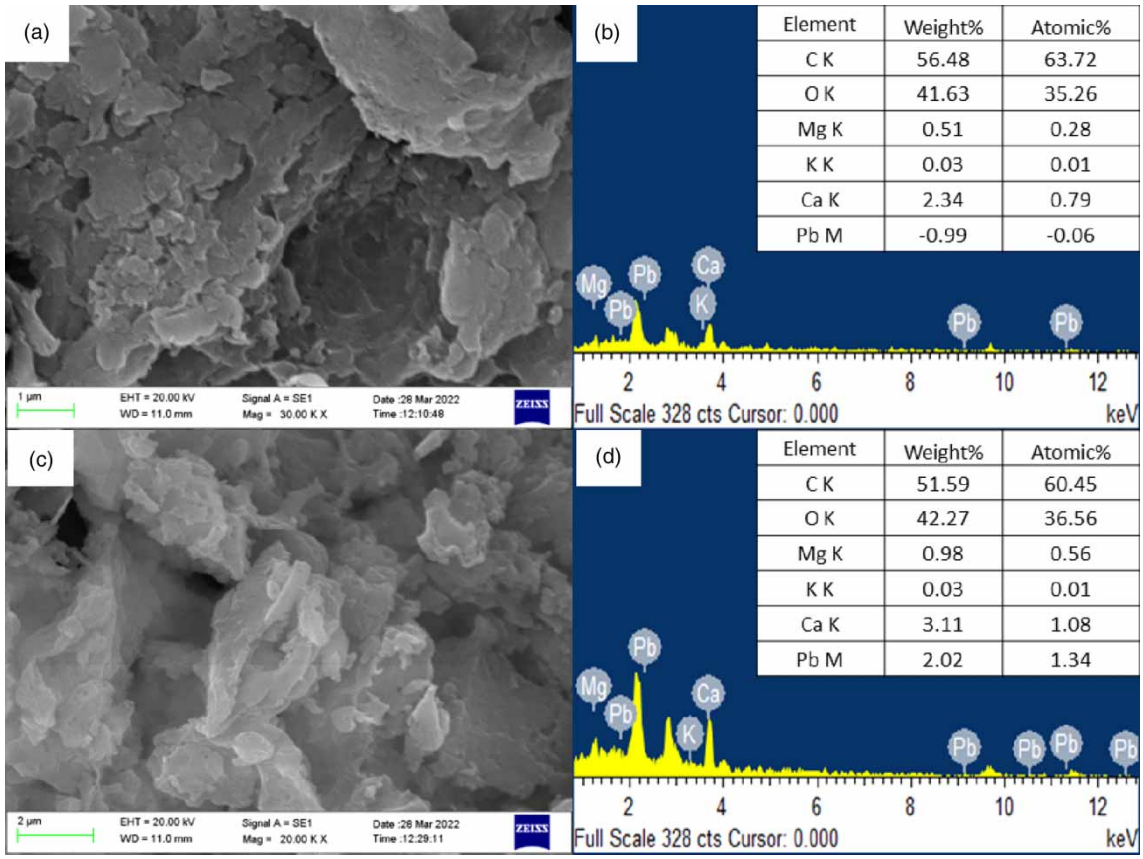

Figure 5 | (a) Raw STG SEM image, (b) lead(II)-adsorbed STG SEM image, (c) EDX analysis of raw STG, (d) EDX analysis of lead(II)-adsorbed STG.

The various elemental compositions of STG before and after the adsorption of lead(II) ions were analysed by EDX analysis as shown in Figure 5(c) and 5(d). The major constituents of the raw STG were found to be only carbon and oxygen. The EDX analysis of STG after lead(II) ions adsorption indicates the existence of lead(II), confirming its attachment to the biosorbent.

Quadratic models for adsorption of lead(II) onto STG

The quadratic model was developed using the CCD design matrix. The matrix was established to investigate the influence of five independent factors (pH, contact time, initial metal ion concentration, stirring speed, and adsorbent dosage of STG). Five levels for different variables were defined (i.e. low (encoded -1), high (encoded $+1$) and rotatable (encoded $\pm\alpha$)). The adsorption uptake capacity and removal efficiency, taken as the main response, were predicted using a polynomial regression equation in which the main, interaction and quadratic effects of the variables were modelled.

The CCD model gives us an experimental run of 32 runs considering all independent variables which will be replicated three times and an average of the results will be taken for the modelling purpose. All the experimental runs are shown in Table 3 with its responses of removal efficiency and adsorption uptake capacity. It is observed during the analysis of the CCD model that the majority of independent process variables affect the responses. The quadratic equation is developed through the CCD design matrix and its main contents area is shown in Table 4. High *F*-value, correlation coefficient (R) tending to 1, low *p*-value and most importantly the results of lack of fill test indicates the high statistical significance of the developed model with high accuracy.

The model *F*-value for percentage removal of 8.70 implies the model is significant. The model *F*-value for uptake capacity of 3.98 implies the model is significant. There is no indication of noise affecting *F*-values.

Low *p*-values for removal efficiency less than 0.05 indicate model terms are significant. Low *p*-values for adsorption uptake capacity less than 0.05 indicate model terms are significant. The Lack-of-Fit *F*-value for % removal of 605.44 implies the Lack-of-Fit is significant. There is only a 0.01% chance that a Lack-of-Fit *F*-value this large could occur due to noise. The Lack-of-Fit *F*-value for uptake capacity of 48,484.97 implies the Lack-of-Fit is significant. There is only a 0.01% chance that a Lack-of-Fit *F*-value this large could occur due to noise.

Table 3 | Central composite design matrix

						% Removal		Uptake capacity	
Run order	pH	Contact time	IMC (mg/l)	Dose (g/l)	Stirring speed (RPM)	Exp.	P	Exp.	P
5	3.25	67.5	16.25	3.25	156.25	68.75	69.53	3.33	4.56
27	5.75	67.5	16.25	3.25	68.75	79.81	81.83	2.73	3.75
23	3.25	142.5	16.25	3.25	68.75	67.12	64.76	3.26	4.40
14	5.75	142.5	16.25	3.25	156.25	90.90	92.95	2.83	3.91
28	3.25	67.5	16.25	7.75	68.75	68.88	69.72	1.40	0.87
6	5.75	67.5	16.25	7.75	156.25	89.69	94.94	1.24	0.63
21	3.25	142.5	16.25	7.75	156.25	74.10	74.98	1.51	1.03
12	5.75	142.5	16.25	7.75	68.75	93.29	95.39	1.22	0.53
20	3.25	67.5	38.75	3.25	68.75	64.01	61.25	7.41	8.53
3	5.75	67.5	38.75	3.25	156.25	76.71	78.35	6.69	7.73
8	3.25	142.5	38.75	3.25	156.25	68.91	66.18	7.98	9.16
24	5.75	142.5	38.75	3.25	68.75	91.09	89.59	6.74	7.71
31	3.25	67.5	38.75	7.75	156.25	69.48	69.95	3.37	2.87
2	5.75	67.5	38.75	7.75	68.75	82.93	84.64	2.91	2.19
16	3.25	142.5	38.75	7.75	68.75	73.46	70.79	3.57	2.99
25	5.75	142.5	38.75	7.75	156.25	96.64	98.38	3.00	2.34
30	2	105	27.5	5.5	112.5	45.42	50.13	2.26	1.48
1	7	105	27.5	5.5	112.5	98.93	92.35	0.29	0.08
4	4.5	30	27.5	5.5	112.5	75.66	71.61	3.34	2.82
9	4.5	180	27.5	5.5	112.5	80.14	82.31	3.53	3.05
26	4.5	105	27.5	1	112.5	74.81	77.17	18.15	14.3
19	4.5	105	27.5	10	112.5	94.98	90.75	2.30	5.19
11	4.5	105	5	5.5	112.5	96.28	91.43	0.77	0.20
29	4.5	105	50	5.5	112.5	82.20	85.18	6.59	6.16
32	4.5	105	27.5	5.5	25	75.50	77.74	3.33	2.96
18	4.5	105	27.5	5.5	200	88.69	84.57	3.91	3.28
17	4.5	105	27.5	5.5	112.5	85.65	85.82	3.78	3.94
15	4.5	105	27.5	5.5	112.5	85.21	85.82	3.76	3.94
7	4.5	105	27.5	5.5	112.5	85.62	85.82	3.78	3.94
10	4.5	105	27.5	5.5	112.5	85.70	85.82	3.78	3.94
22	4.5	105	27.5	5.5	112.5	85.74	85.82	3.78	3.94
13	4.5	105	27.5	5.5	112.5	85.15	85.82	3.76	3.94

The regression analysis of CCD afforded the following second-order polynomial equation for lead(II) ion in terms of % removal:

$$\begin{aligned} Y = & 85.82 + 10.56 \times A + 2.67 \times B + 3.40 \times C - 1.56 \times D + 1.71 \times E + 1.89 \times A \times B \\ & + 4330 \times A \times C - 0.2081 \times A \times D - 0.0593 \times A \times E - 0.1385 \times B \times C + 1.17 \times B \times D \\ & - 0.2120 \times B \times E + 0.1519 \times C \times D + 0.5084 \times C \times E - 0.8814 \times D \times E - 3.65 \times A^2 \\ & - 2.21 \times B^2 - 0.4653 \times C^2 + 0.6211 \times D^2 - 1.17 \times E^2 \end{aligned} \quad (4)$$

Table 4 | ANOVA for quadratic model: (a) response 1: removal and (b) response 2: uptake capacity

Source	Sum of squares	*df*	Mean square	*F*-value	*p*-value	
(a) Response 1: Removal						
Model	3,903.06	20	195.15	8.70	0.0004	significant
A-pH	2,674.74	1	2,674.74	119.28	< 0.0001	
B-Contact Time	171.73	1	171.73	7.66	0.0183	
C-Adsorbent Dose	276.82	1	276.82	12.34	0.0049	
D-Intial Metal Ion Concentration	58.54	1	58.54	2.61	0.1345	
E-Stirring Speed	69.90	1	69.90	3.12	0.1052	
AB	57.29	1	57.29	2.55	0.1383	
AC	3.00	1	3.00	0.1338	0.7215	
AD	0.6932	1	0.6932	0.0309	0.8636	
AE	0.0562	1	0.0562	0.0025	0.9610	
BC	0.3069	1	0.3069	0.0137	0.9090	
BD	21.82	1	21.82	0.9732	0.3451	
BE	0.7191	1	0.7191	0.0321	0.8611	
CD	0.3692	1	0.3692	0.0165	0.9002	
CE	4.14	1	4.14	0.1844	0.6759	
DE	12.43	1	12.43	0.5543	0.4722	
A^2	389.77	1	389.77	17.38	0.0016	
B^2	143.83	1	143.83	6.41	0.0278	
C^2	6.35	1	6.35	0.2832	0.6052	
D^2	11.31	1	11.31	0.5046	0.4923	
E^2	39.89	1	39.89	1.78	0.2093	
Residual	246.67	11	22.42			
Lack-of-Fit	246.33	6	41.06	605.44	< 0.0001	significant
Pure Error	0.3391	5	0.0678			
Cor Total	4149.73	31				
(b) Response 2: Uptake Capacity						
Model	277.16	20	13.86	3.98	0.0113	significant
A – pH	2.95	1	2.95	0.8456	0.3775	
B – Contact time	0.0822	1	0.0822	0.0236	0.8807	
C – Adsorbent dose	123.53	1	123.53	35.45	< 0.0001	
D – Intial metal ion concentration	53.33	1	53.33	15.30	0.0024	
E – Stirring speed	0.1471	1	0.1471	0.0422	0.8409	
AB	0.0200	1	0.0200	0.0057	0.9409	
AC	0.1410	1	0.1410	0.0405	0.8443	
AD	0.1442	1	0.1442	0.0414	0.8425	
AE	0.0101	1	0.0101	0.0029	0.9581	
BC	0.0044	1	0.0044	0.0013	0.9723	
BD	0.0390	1	0.0390	0.0112	0.9176	
BE	0.0080	1	0.0080	0.0023	0.9628	
CD	5.27	1	5.27	1.51	0.2444	
CE	0.0285	1	0.0285	0.0082	0.9296	

(*Continued.*)

Table 4 | Continued

Source	Sum of squares	*df*	Mean square	*F*-value	*p*-value	
DE	0.0008	1	0.0008	0.0002	0.9884	
A^2	18.32	1	18.32	5.26	0.0426	
B^2	1.84	1	1.84	0.5287	0.4824	
C^2	61.40	1	61.40	17.62	0.0015	
D^2	1.06	1	1.06	0.3041	0.5924	
E^2	1.23	1	1.23	0.3516	0.5652	
Residual	38.33	11	3.48			
Lack-of-Fit	38.33	6	6.39	48,484.97	< 0.0001	significant
Pure error	0.0007	5	0.0001			
Cor total	315.49	31				

The regression analysis of CCD afforded the following second-order polynomial equation for lead(II) ion in terms of uptake capacity:

$$\begin{aligned} Y = {} & 3.94 - 0.3504 \times A + 0.0585 \times B - 2.27 \times C + 1.49 \times D + 0.0783 \times E - 0.0354 \times A \times B \\ & + 0.0939 \times A \times C - 0.0949 \times A \times D - 0.0251 \times A \times E - 0.0166 \times B \times C + 0.0494 \times B \times D \\ & + 0.0223 \times B \times E - 0.5793 \times C \times D - 0.0422 \times C \times E + 0.0069 \times D \times E - 0.7903 \times A^2 \\ & - 0.2506 \times B^2 + 1.45 \times C^2 - 0.1901 \times D^2 - 0.2044 \times E^2 \end{aligned} \quad (5)$$

ANOVA gives us the possible interactions between independent variables as represented in Table 4(a) and (b). The pH, stirring speed, initial ion concentration, contact time and adsorbent dosage affect both the adsorption capacity and removal efficiency. Figure 6(a) and 6(b) show the graphs of actual versus predicted data obtained from the adsorption of lead(II) onto STG. The derived quadratic equations using the CCD matrix were found to be suitable for predicting independent process variables' influence on removal efficiency as well as uptake capacity of lead(II) adsorption onto STG.

Effect of various factors on the adsorption of lead(II) onto STG using RSM

3D surface plots were provided by the quadratic model, representing two independent process variables with their predicted responses either removal efficiency or uptake capacity. These 3D plots are analysed to pinpoint the optimal or near-optimal adsorption areas. The overall effect of various parameters interacting with pH was shown in Figure 7(a)–7(d). As the pH increases the removal efficiency tends to increase. The adsorption appears to be more favoured as pH approaches around 5 when both the responses are combined and analysed.

Figure 8(a)–8(c) illustrates the relationship between contact time with other independent variables. It shows as the contact time increases there is an increase in removal efficiency. Similarly Figure 9(a)–9(b) illustrates the relationship between adsorbent dose with other independent variables, it shows that with the increase in adsorbent dose, there tends to increased removal efficiency of the system. Figure 9(c) represents a relationship between stirring speed and initial metal ion concentration. It shows as IMC increases removal efficiency decrease with the decrease in stirring speed.

The desirability plot in Figure 10 enabled us to visualize the desirability for the process variable and output. It is seen from Figure 10 that the desirability value was 1 for the individual and a combination of all process variables at a maximum of 0.619 was developed from STG for lead(II) removal.

Influence of various parameters

Effect of pH

In the present study, the influence of pH on the adsorption capacity and % removal efficiency were studied. The pH in the range of 2.0–7.0 was adjusted using dilute acid/base. The initial pH value of the prepared aqueous solution containing lead(II)

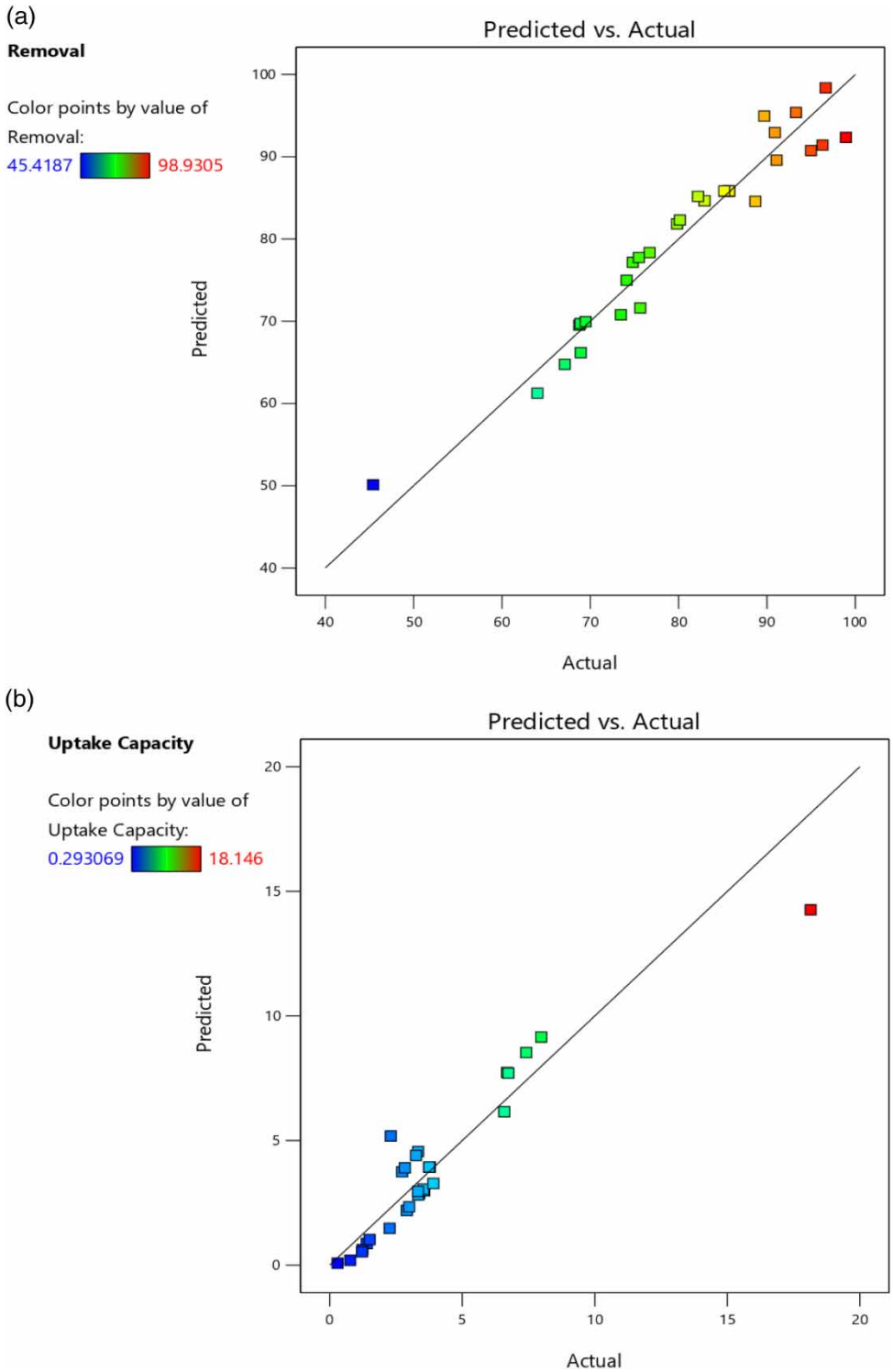

Figure 6 | (a): Actual vs. predicted values in terms of removal efficiency and (b) actual vs. predicted values in terms of uptake capacity.

ions was found to be around 4.2 ± 0.4. For detailed estimation of optimum pH, three different adsorbent doses were considered for the experiment (low dose of 1 g/l, average dose 2.5 g/l, and high dose 5 g/l), and four different initial metal ion concentrations were considered (5, 10, and 15 mg/l). Other parameters remain constant, i.e. contact time of 90 mins, shaker speed of 150 rpm.

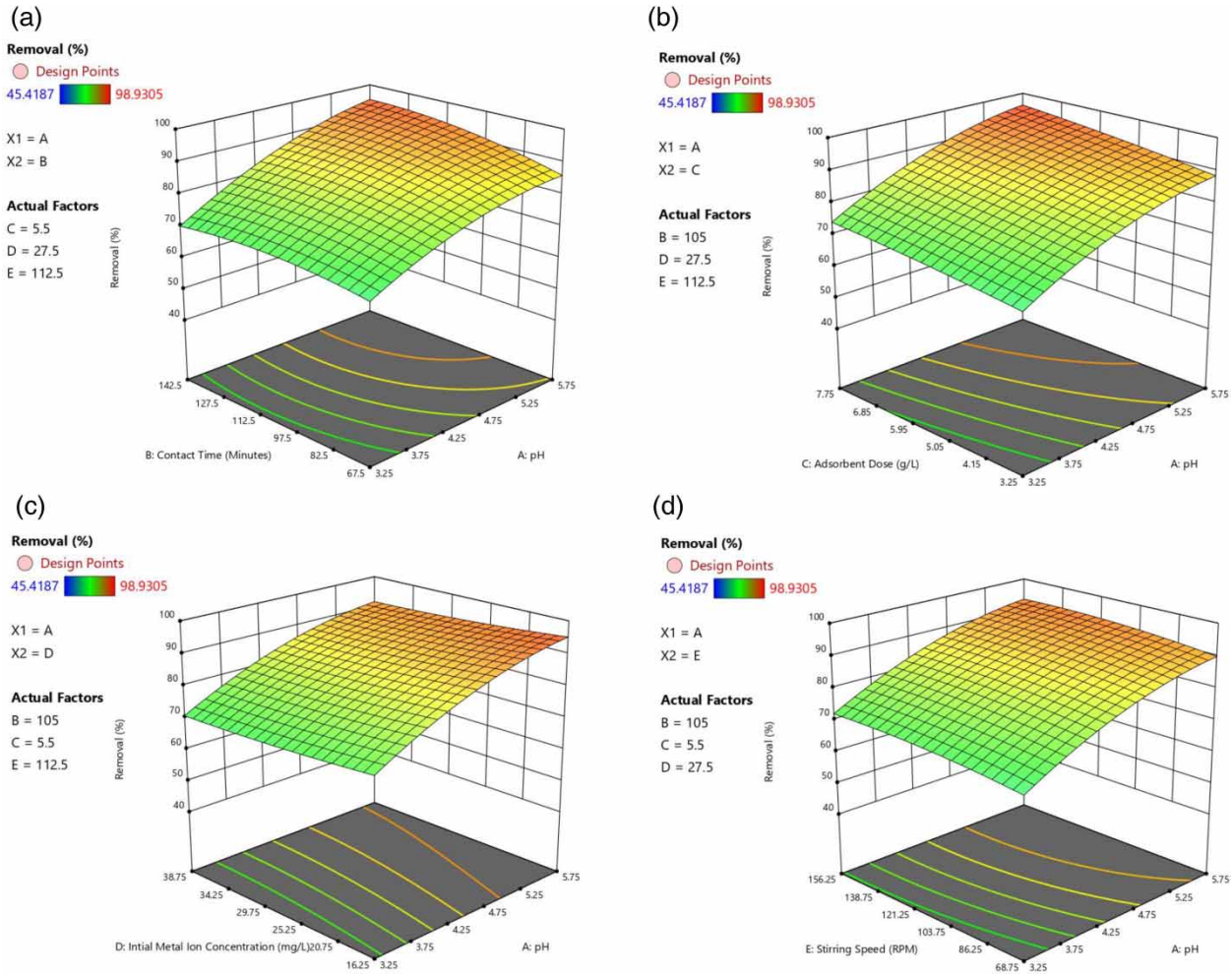

Figure 7 | 3D surface plots showing the effect of various factors w.r.t removal efficiency: (a) pH vs. CT, (b) pH vs. AD, (c) pH vs. IMC, and (d) pH vs. SS.

In an aqueous solution at pH $\geq$ 7 the dissolution of lead(II) ions cannot be possible, therefore assessment of lead(II) contamination and its removal by STG can be misleading. At pH = 7 and above, the hydroxide precipitation of lead(II) ions may mislead adsorption results. Therefore, the batch experiment for evaluation of the influence of pH was conducted in the pH range of 2–7. Precipitation of lead(II) ions can be analysed by the Pourbaix diagram. By this diagram, we know that the lead(II) ions precipitated as Pb $(OH)_2$ at pH > 6. However, at pH < 6, the removal of the lead(II) ions may be governed by other applied mechanisms. As can be seen from Figures 6(a) and 6(b), the removal percentage of the lead(II) ions was low when the pH was 2 or 3 as acidic conditions favour undissociated forms of functional groups. It was noted from the Figures 11(a) and 11(b), that when pH was increased to 4–5, the removal percentage of the Pb ions increased significantly from 33.54% to 84.99% at an initial concentration of 15 ppm, contact time 90 min and adsorbent dose of 0.1 g/100 ml. Further increasing pH to 6 the removal efficiency increased to 89.93%. A similar phenomenon was observed for all other variations as seen from the Figure 11(a) and 11(b).

When we analysed the Figure 11(a) and 11(b) with respect to both adsorption capacity and removal efficiency we get our optimum value of pH, i.e. pH = 5. At pH 5, the uptake capacity was found to be maximum with very good % removal efficiency.

Further increasing pH from 5 to 7 increases our removal percentage but decreases adsorption uptake. When the effects of pH value on the removal percentage and adsorption uptake of the metals were examined simultaneously, it was found that the optimum value for Pb was pH 4.96 $\pm$ 0.12. At lower pH values the H+ ions compete with metal cations for the electrostatic surface charges in the system decreasing the percentage of sorption. These outcomes regarding the pH amount are also parallel to various studies that used acidic pH. The experimental results showed that the maximum removal percentage of Pb

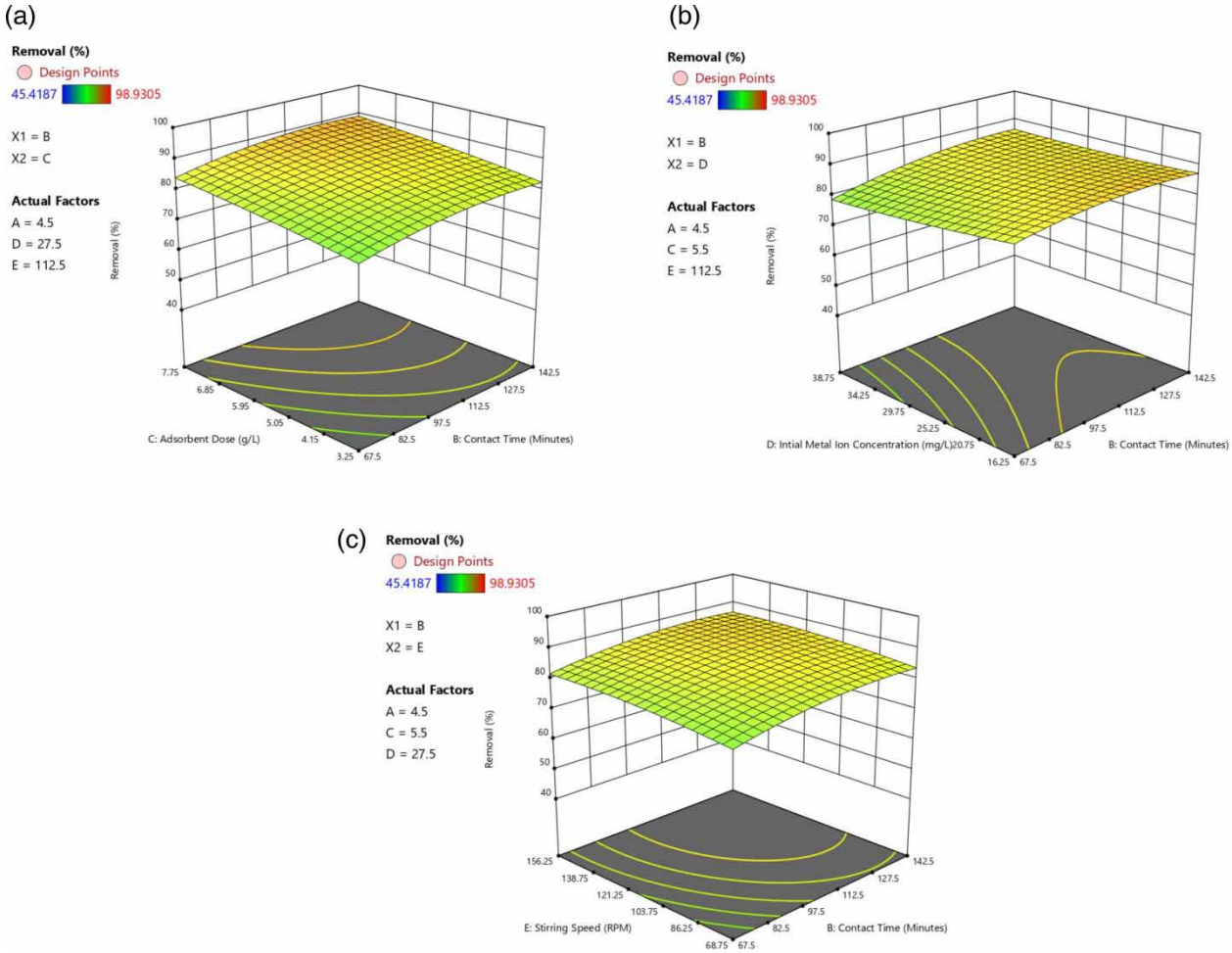

Figure 8 | 3D surface plots showing the effect of various factors w.r.t removal efficiency: (a) CT vs. AD, (b) CT vs. IMC, and (c) CT vs. SS.

is found to be 96.67% at the optimum pH, $C_o = 5$ ppm, contact time = 90 min, adsorbent dose = 0.5 g/100 ml, stirring speed = 150 rpm.

Effect of contact time

The adsorption capacities and removal efficiency of STG for different contact times in the range of 30–180 min were analysed at initial metal concentrations of 5 and 15 mg/l at three different STG dosages, i.e. 01.g/100 ml, 0.25 g/100 ml and 0.5 g/100 ml. As can be deduced from Figure 12, the removal efficiencies of the lead(II) ions at the start are very sharp and then increased up to approximately 90 min, after which it is almost constant. The maximum removal efficiency was reached at a high dose of 0.5 g/100 ml and at a lower initial metal ion concentration of 5 mg/l, and it is found to be 94.33% around the 90 min mark. It is to be noted that in all the experiments metal uptake increases up to 90 min and after that, it is almost constant.

Effect of initial metal ions concentrations

The adsorption experiment was carried out at room temperature by varying the initial metal ions concentration from 5 to 50 mg/l to study the effect of the initial metal ion concentration. Other parameters considered are optimum pH and optimum contact time found in previous stages, three different adsorbent doses considered (1, 2.5, and 5 g/l) shaking speed of 150 rpm. The influence of initial metal ions concentration on removal efficiency and adsorption uptake capacity is shown in Figure 13. When we vary the initial metal ion concentration of lead(II) from 5 to 50 mg/l the removal efficiency decreases slightly, and adsorption uptake increase rapidly for a particular dosage of STG (adsorbent). For STG dosage of 0.5 g/100 ml when initial

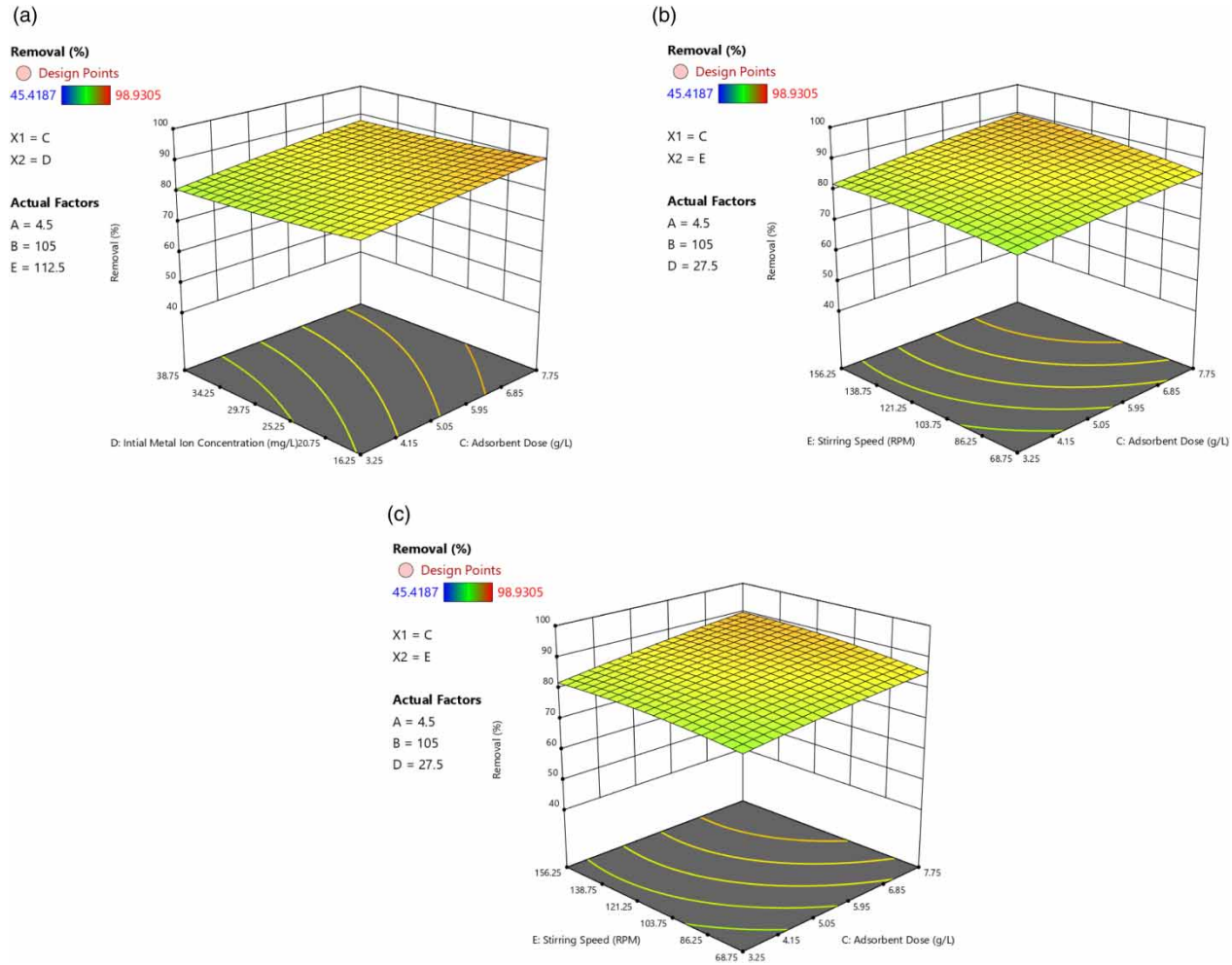

Figure 9 | 3D surface plots showing the effect of various factors w.r.t removal efficiency: (a) AD vs. IMC, (b) AD vs. SS, and (c) SS vs. IMC.

lead(II) ion concentration increases from 5 to 50 mg/l the removal efficiency decreases from 97.32 to 91.95%, and adsorption uptake increases from 0.7928 to 7.3428 mg/g. The phenomenon is also observed in other variations.

Effect of adsorbent dose

To achieve the maximum efficiency of the prepared adsorbent (i.e. STG) for Pb (II), the adsorbent dose was varied from 1 to 5 g/l at room temperature. Other parameters considered are optimum pH and optimum contact time found in previous stages, initial metal ion concentration of 5 and 15 mg/l, and shaking speed of 150 rpm. As can be seen from Figure 14 when we increase STW dosage from 0.1 g/100 ml to 1 g/100 ml, we observe that lead(II) ions removal efficiency increased to 98.24% from 89.82%, when the initial metal ions concentration is 5 mg/l with other optimum parameters (i.e. pH around 5, contact time = 90 min, stirring speed = 150 rpm, at room temp.) for a particular particle size range used of prepared adsorbent STG (i.e. 600–75 μm). The trend shown in the removal efficiency increment is due to increases in the retention capacity of the active surface of STG for heavy metal considered.

Effect of particle size

The influence of STG particle size on removal efficiency and metal uptake capacity can be deduced from Figure 15. As we can see, the smaller the particle size of STG the more efficient the removal of lead(II) ions from the aqueous solution. Lead(II) ions removal efficiency increases from 85.69 to 92.68% as particle size decreases from the range of >1,180 150–75 μm. Other

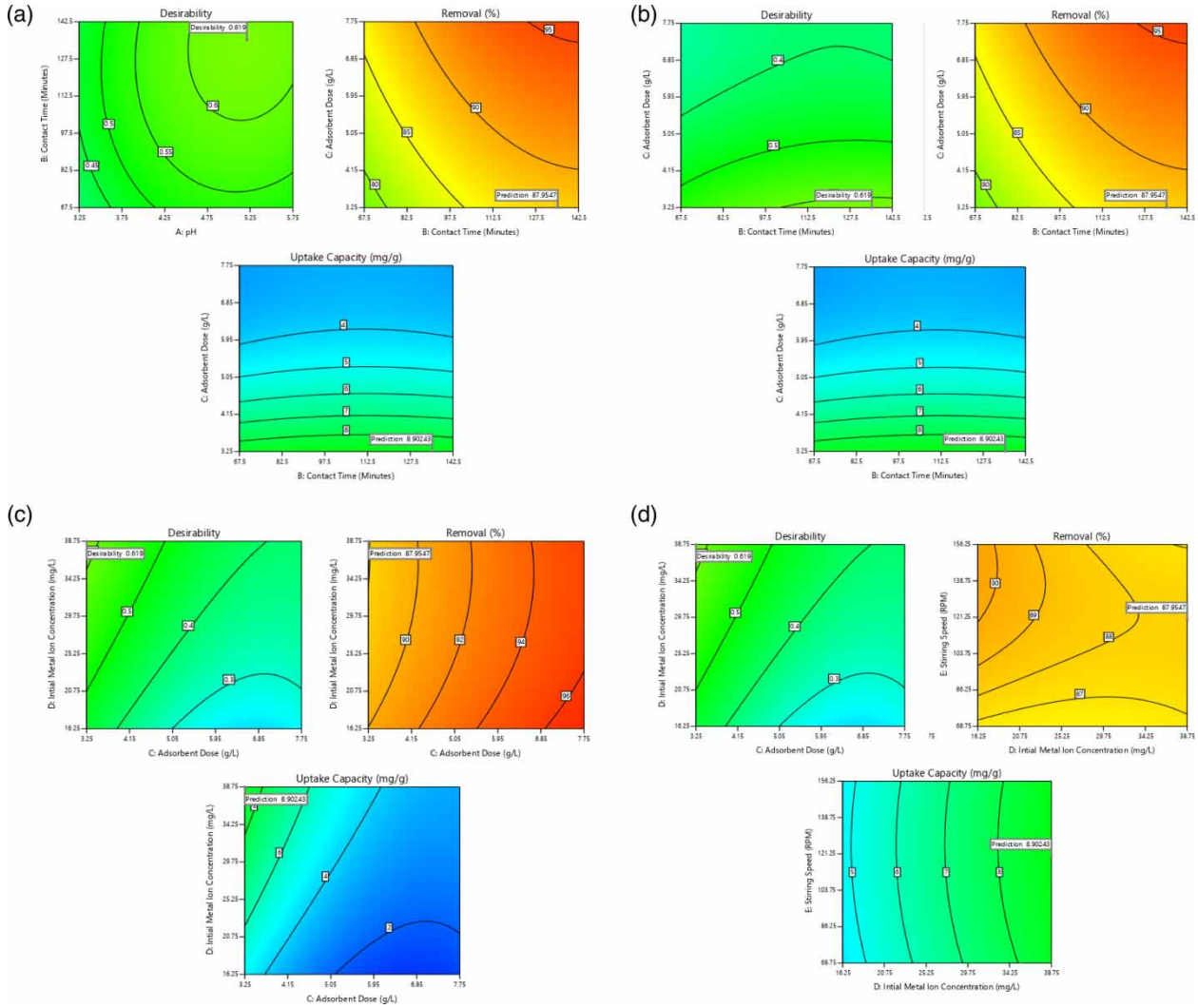

Figure 10 | Desirability plots shows various independent variables' interaction: (a) pH vs. CT, (b) CT vs. AD, (c) AD vs. IMC, and (d) IMC vs. SS.

parameters are optimum as found through different batch study experiments, i.e. pH around 5, contact time = 90 min, stirring speed = 150 rpm, initial metal ion concentrations = 15 mg/l, adsorbent dosage of 0.5 g/100 ml at room temp.

Effect of stirring speed

As we can observe from Figure 16, as the stirring speed of the rotary shaker was increased during our various batch study experiments there is some increment observed in the removal efficiency of the STG in removing lead(II) ions removal from aqueous solution. The maximum removal efficiency was observed at 150 rpm which is used during our various batch study experiments.

Adsorption isotherm models

The relationship between the lead(II) ions in the prepared synthetic wastewater with prepared adsorbent STG was established using the Freundlich, Langmuir, Temkin and Dubinin–Radushkevich (D–R) isotherms. The isotherms governing parameters of Freundlich (F) (Equation (6)), Langmuir (L) (Equation (7)), were defined as:

$$Q_e = Kf\sqrt[n]{C_e} \tag{6}$$

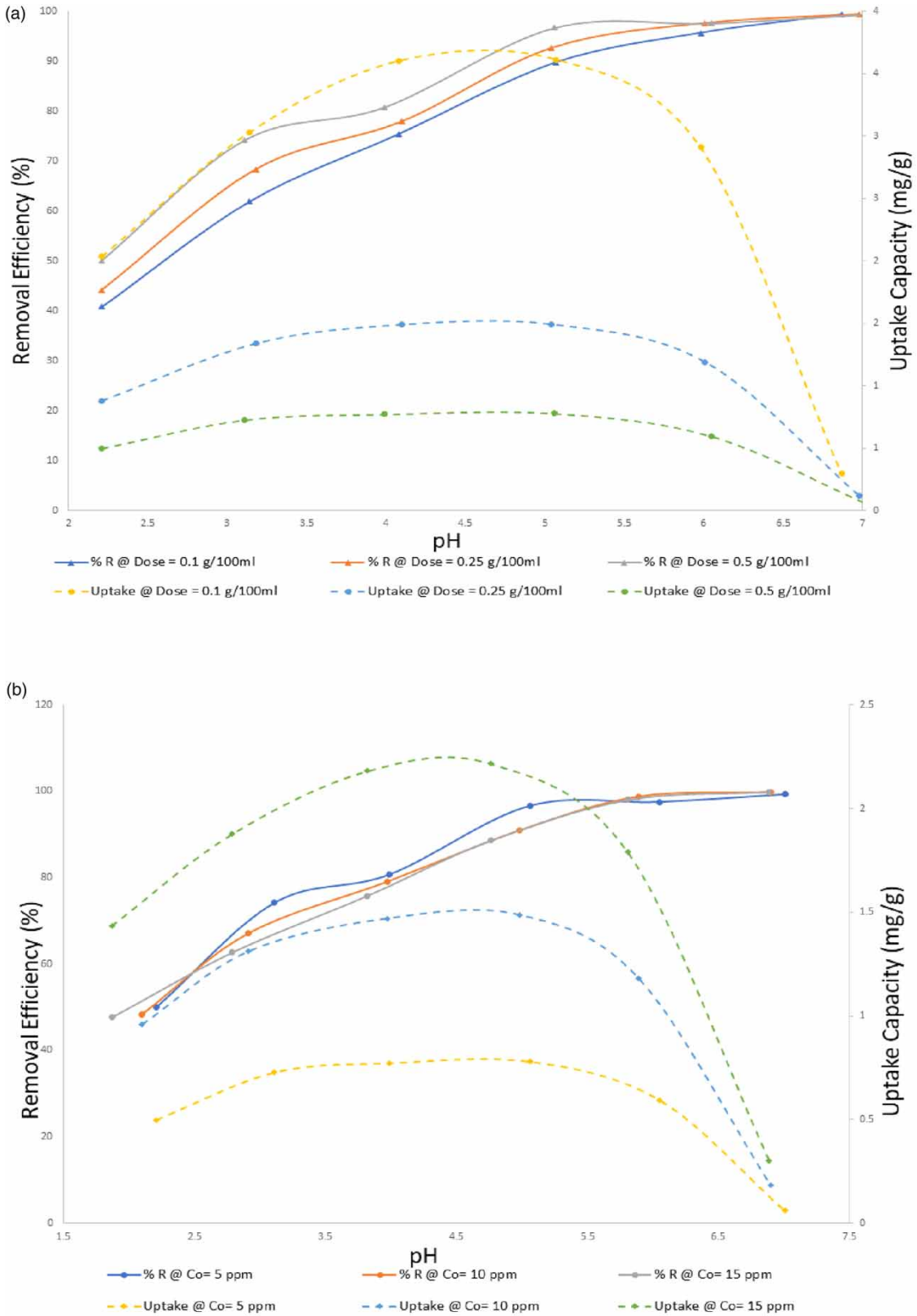

Figure 11 | (a) Effect of pH on lead(II) removal efficiency and uptake capacity at $C_o = 5$ ppm, contact time = 90 min, stirring speed = 150 rpm, temp. = 25 °C. (b) Effect of pH on lead(II) removal efficiency and uptake capacity at STG dose = 0.5 g/100 ml, contact time = 90 min, stirring speed = 150 rpm, temp. = 25 °C.

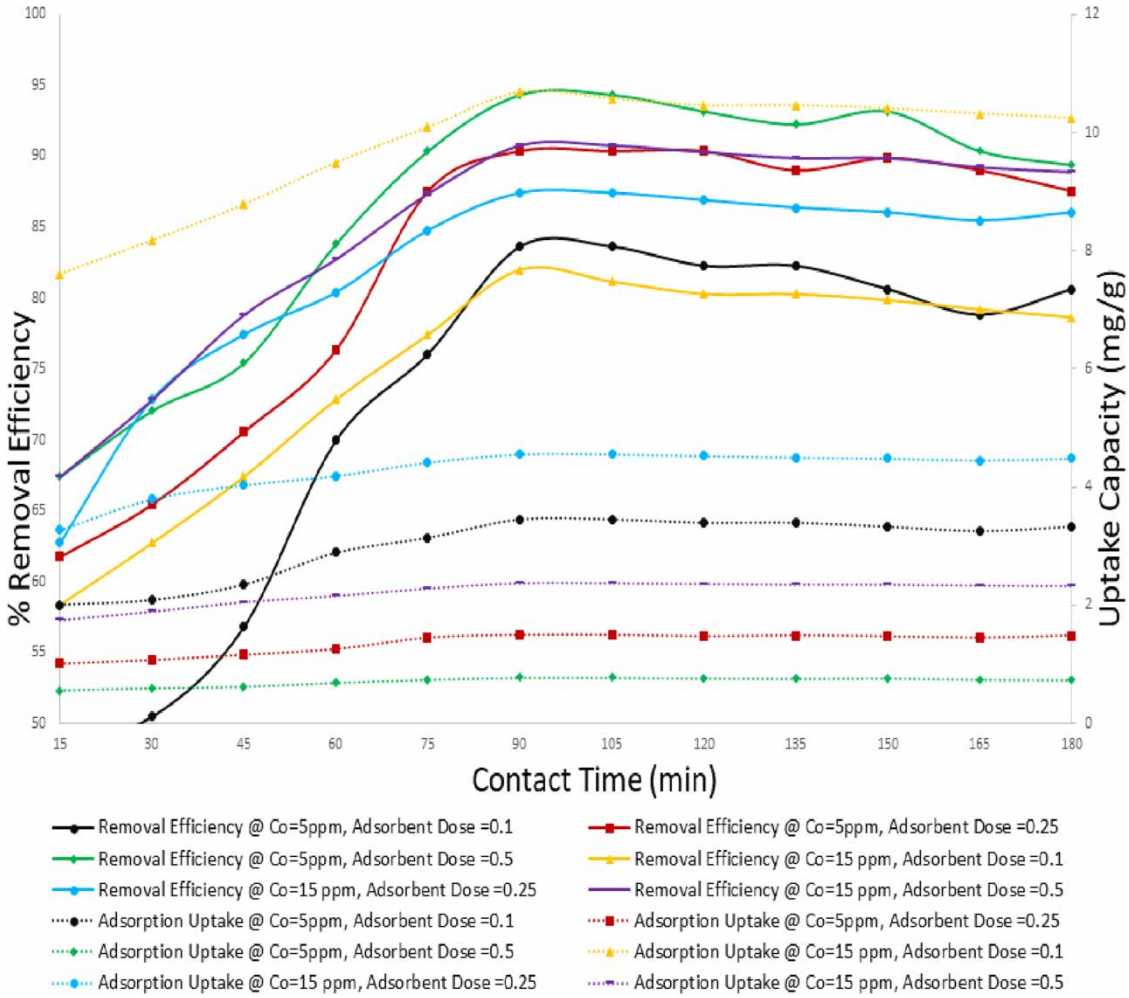

Figure 12 | Effect of the contact time on lead(II) removal efficiency and uptake capacity.

$$Q_e = \frac{Q_m K_L C_e}{1 + K_L C_e} \tag{7}$$

Here, C_e refers to the balance amount of lead ions (mg/l). Q_e refers to the adsorption capacity of adsorbent STG at equilibrium in mg/g. Q_m refers to the the maximum adsorption capacity of adsorbent STG in mg/g, K_L refers to the Langmuir constant (L/mg). K_F and $1/n$ refer to the Freundlich constants. Kinetics models used will give a clear indication about the changes in the adsorption mechanism within a stipulated time-period and provide significant information required for the experimental setup.

The effects of indirect interactions between adsorbate and adsorbent will be investigated by the isotherm model suggested by Temkin and Pyzhev. They suggested that these adsorbate/adsorbent interactions will decrease linearly the heat of adsorption in the adsorbate layer in contact as it covers it. The Temkin isotherm equation will follow the following form:

$$Q_e = \frac{RT}{b_T} LN\,(A_T C_e) \tag{8}$$

Investigation of porosity, characteristics of adsorption and apparent free energy will be done using D–R isotherm model.

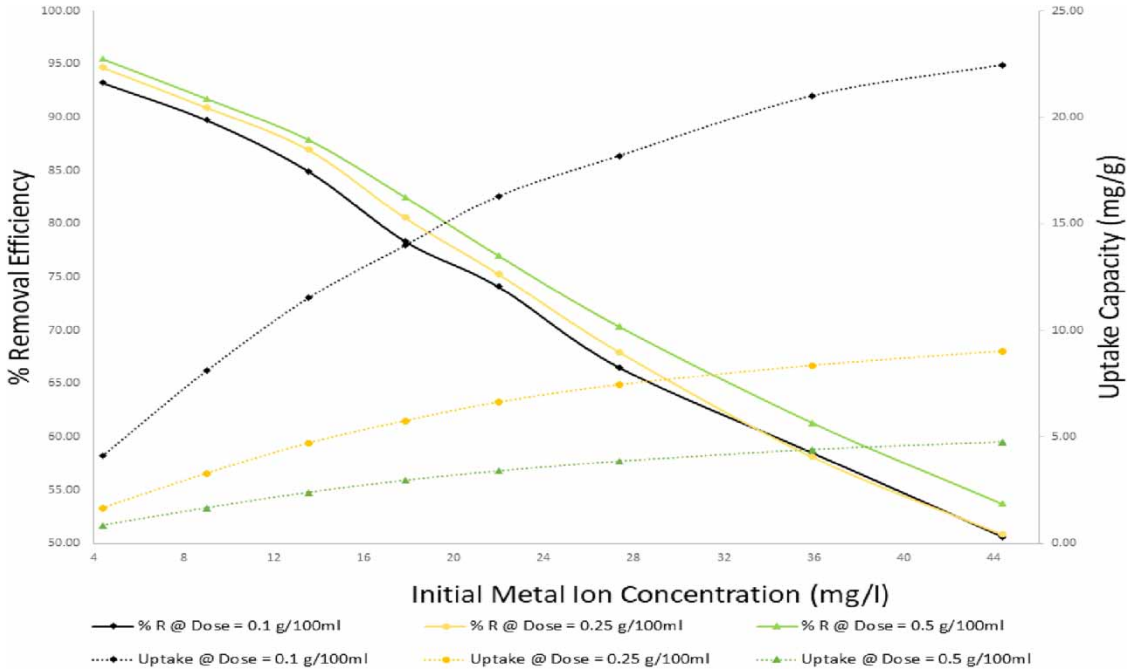

Figure 13 | Effect of the initial metal ion concentration on lead(II) removal efficiency and uptake capacity.

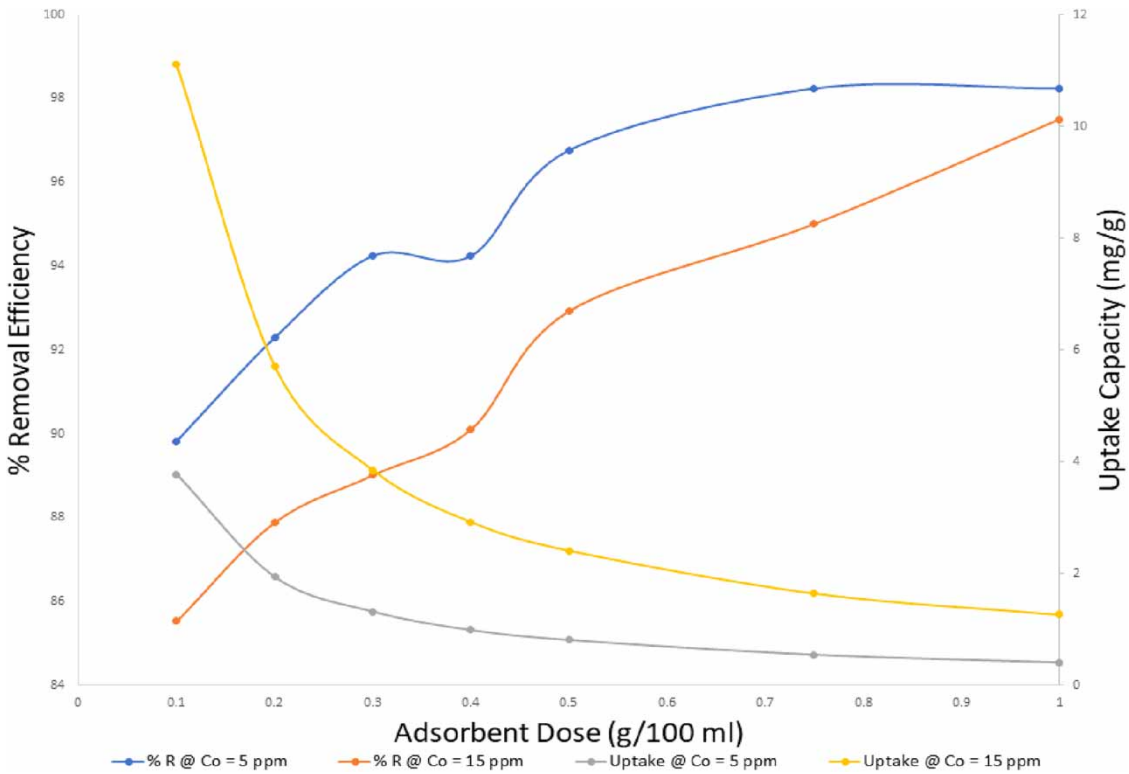

Figure 14 | Effect of the adsorbent dose on lead(II) removal efficiency and uptake capacity.

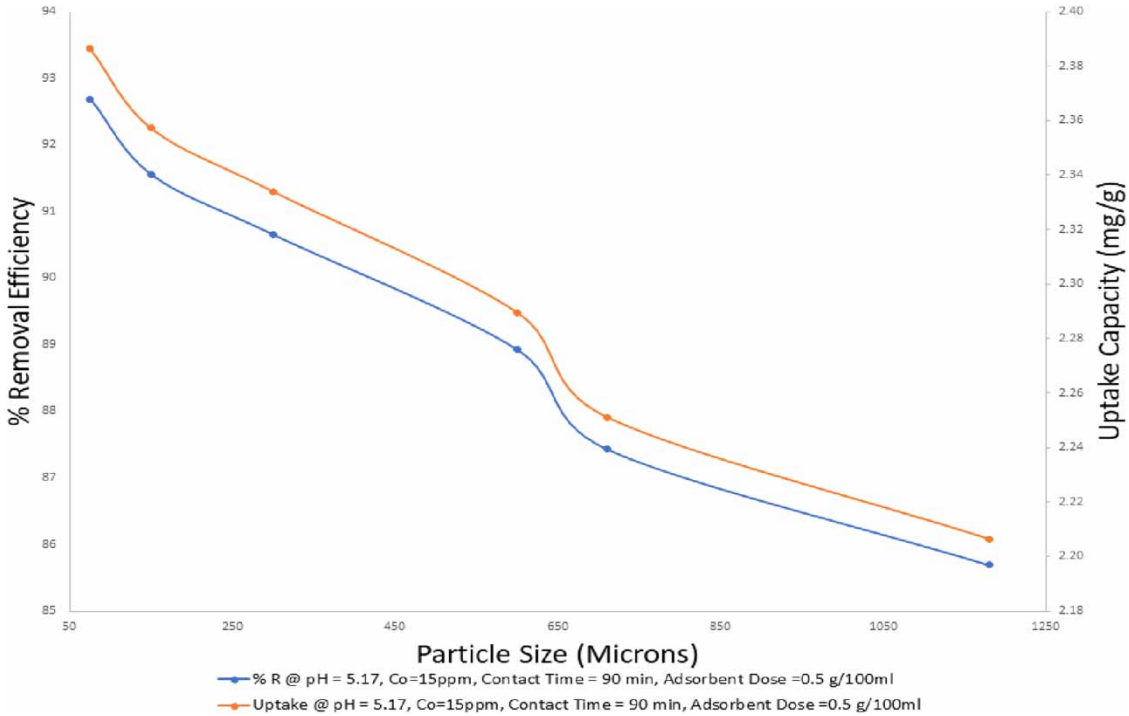

Figure 15 | Effect of the particle size on lead(II) efficiency and uptake capacity.

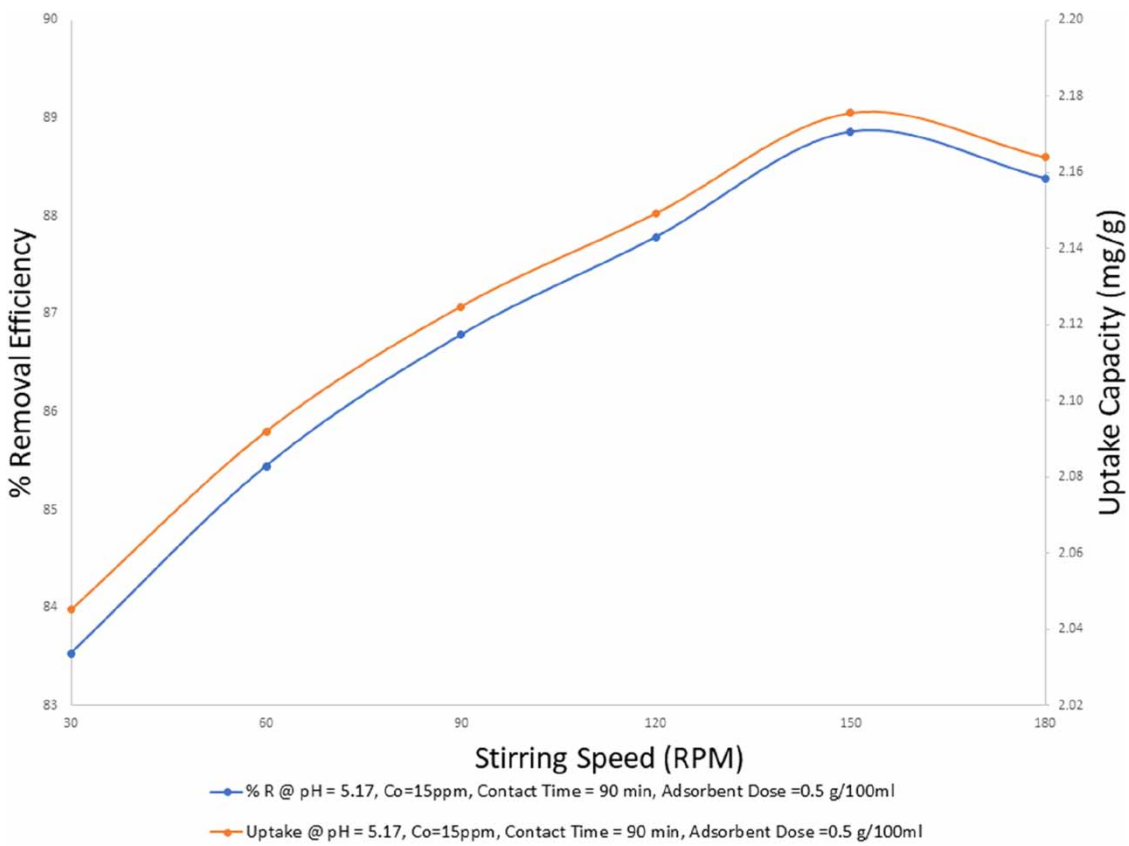

Figure 16 | Effect of the stirring speed on lead(II) removal efficiency and uptake capacity.

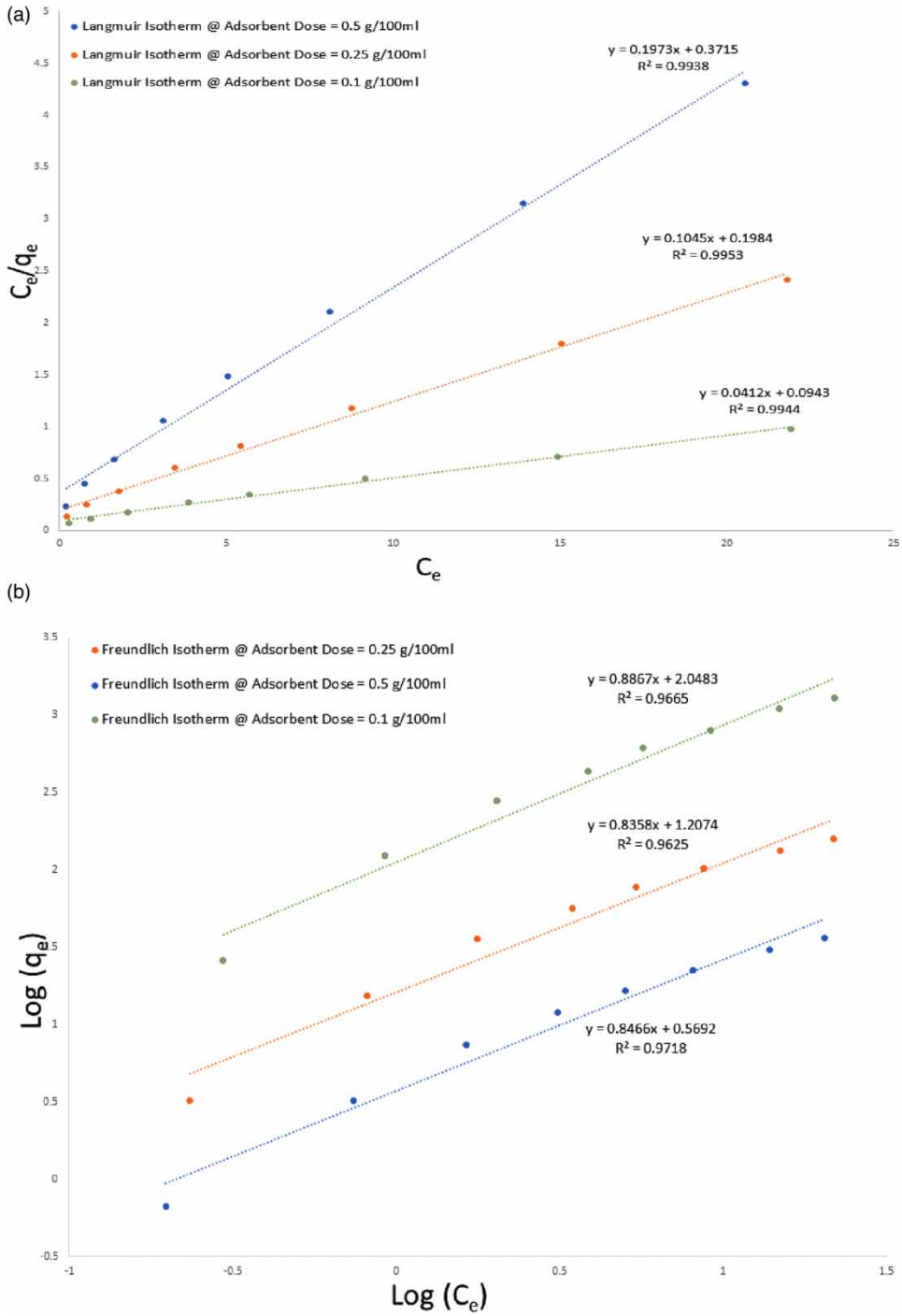

Figure 17 | (a) Langmuir isotherm, (b) Freundlich isotherm, (c) Temkin isotherm, and (d) D–R isotherm. (*continued.*).

The D–R isotherm was applied in the following form:

$$q_e = Q_m \exp(-K\varepsilon^2) \tag{9}$$

The linear form of D–R isotherm is:

$$lnq_e = lnQ_m - K\varepsilon^2 \tag{10}$$

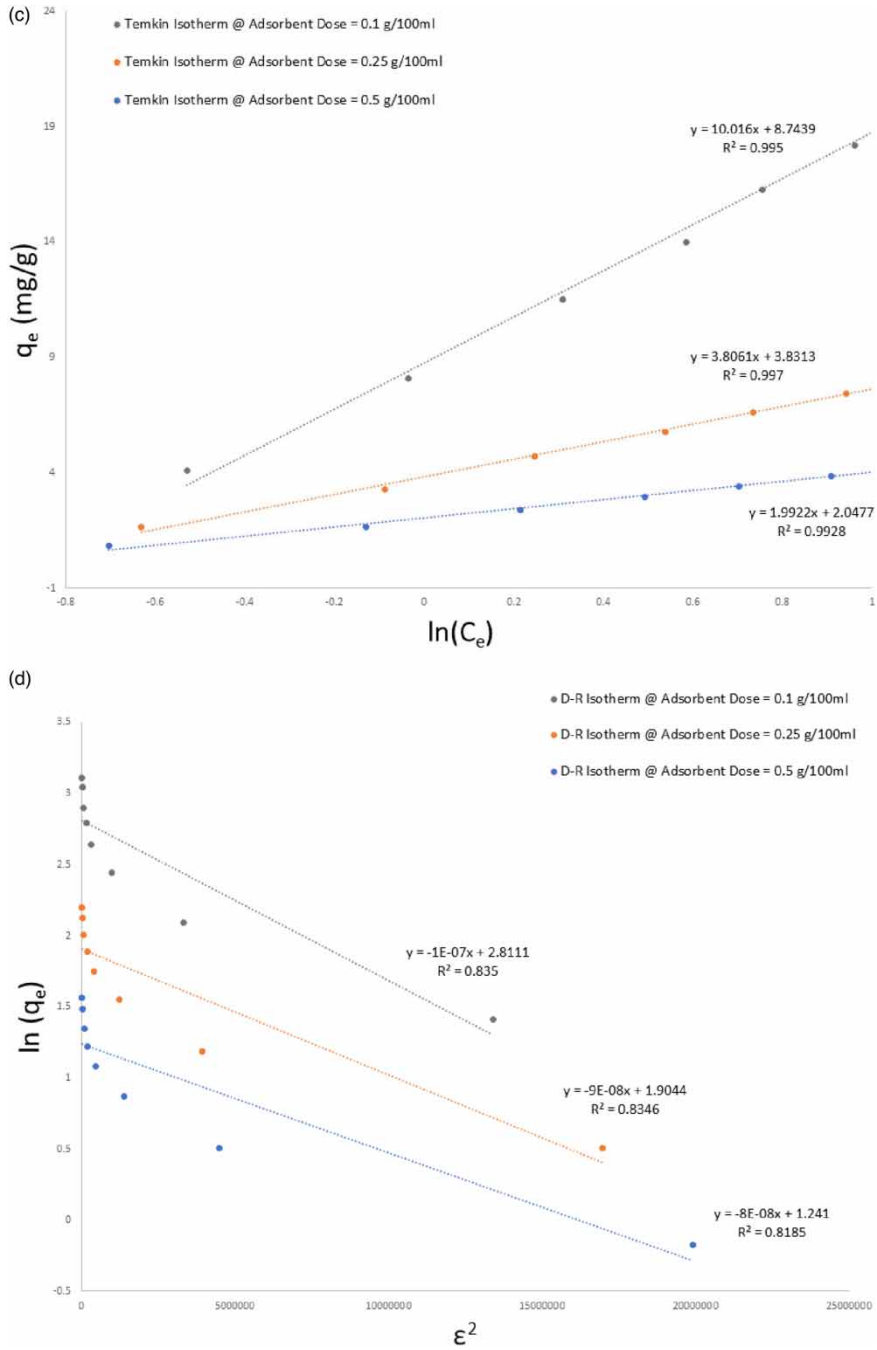

Figure 17 | Continued.

where K is D–R constant, Q_m is the adsorption saturation capacity, ε is the Polanyi potential, ε can be calculated by:

$$\varepsilon = RTln\left(1 + \frac{1}{C_e}\right) \tag{11}$$

The mean free energy of sorption (E) will be calculated using D–R constant given by:

$$E = \frac{1}{\sqrt{2K}} \tag{12}$$

By looking at Figure 17(a)–17(d) we can see the plot between initial lead(II) ion concentration and removal efficiency at optimum conditions (i.e. pH around 5, contact time = 90 min, stirring speed = 150 rpm, room temp.) showing various isotherms at STG dosage of 0.1 g/100 ml, 0.25 g/100 ml, and 0.5 g/100 ml.

The linear Langmuir isotherm plots STG is shown in Figure 17(a). R^2 greater than 0.99 is a good indication of the suitability of lead(II) ions adsorption onto STG. Using Langmuir, the isotherm maximum adsorption capacity is found to be 24.272 mg/g. R_L is of utmost importance which indicates the condition of adsorption onto adsorbent. R_L greater than 1 is unfavourable and signifies non-optimum adsorption, linear adsorption for $R_L = 1$, and favourable optimum adsorption occurs when R_L values lie in between 0,1. Now in our present study, we found $R_L = 0.1444$ which indicates optimum lead(II) adsorption onto STG. All the calculated data are presented in Table 5.

When we study the Freundlich isotherm in its linear form it also shows a good correlation coefficient $R^2 = 0.9665$ which suggests STG possesses high affinity and high adsorption capacity. As $1/n < 1$ it suggests optimum adsorption condition, it also indicates multilayer adsorption onto heterogeneous surfaces.

Temkin isotherm model investigation shows a very good correlation coefficient of $R^2 > 0.99$, values of equation parameters $b_T = 247.486$ and $A_T = 7.4644$. The value of the correlation coefficient for the D–R model is low ($R^2 = 0.835$) as compared to the other models, suggesting that the data is not fitted into the D–R isotherm models. Moreover, the value of maximum adsorption capacity calculated using the D–R isotherm model is not close to the value calculated using the Langmuir isotherm model.

Adsorption kinetics models

We have adopted the use of four conventional kinetic models, namely pseudo-first-order, pseudo-second-order, intraparticle diffusion and Elovich kinetics models, to investigate the adsorption mechanism according to the experimental data gathered. The equations for the PFO and PSO models can be expressed as follows, in the given order:

$$\log (Q_e - Q_t) = Log(Q_e) - k_1 * 2.303t \tag{13}$$

$$\frac{t}{Q_t} = \frac{1}{k_2 Q_e^2} + \frac{t}{Q_e} \tag{14}$$

In the aforementioned equation Q_e measured in mg/g, is the adsorption capacity of STG at equilibrium and Q_t measured in mg/g is the adsorption capacity of STG at a certain time t; k_1 and k_2 are the pseudo-first-order rate constant and pseudo-second-order rate constant, respectively. The slope and intercept from the linear plot of ln $(Q_e - Q_t)$ versus t as defined by the pseudo-first-order model will provide the values of k_1 and Q_e while in the case of the pseudo-second-order model, the linear plot of t/Q_t versus t will define the values of Q_e and k_2.

Table 5 | Isotherms study parameters of lead(II) adsorption on STG at adsorbent dose = 0.1 g/100 ml and other optimum parameters

Model	Parameters	Values
Langmuir isotherm	q_m (mg/g)	24.272
	K_L (L g^{-1})	0.4369
	R^2	0.994
	R_L	0.1444
Freundlich isotherm	K_F (mg/g)	111.764
	n	1.1278
	$1/n$	0.8867
	R^2	0.9665
Temkin isotherm	A_T	7.464
	b_T	247.486
	R^2	0.995
D–R isotherm	q_m (mg/g)	16.628
	K (mol^2/K^2J^2)	0.0000001
	R^2	0.835
	E (KJ/mol)	2,236.07

The intraparticle diffusion model is needed to investigate the adsorption diffusion mechanism based on the principle suggested by Weber and Morris. According to the principle:

$$q_t = k_{pi} t^{1/2} + C_i \tag{15}$$

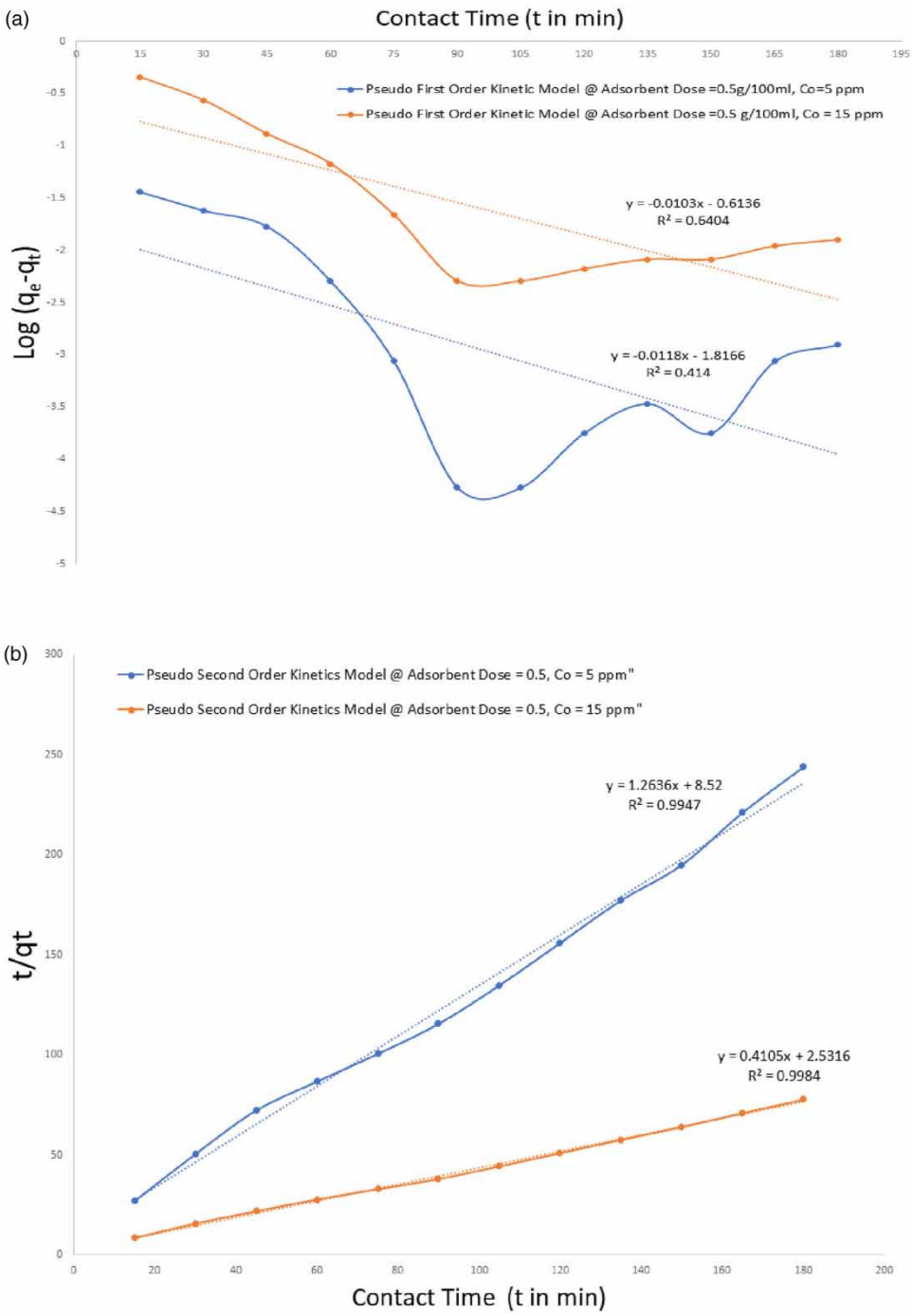

Figure 18 | (a) Pseudo-first-order kinetics, (b) pseudo-second-order kinetics (c) intraparticle diffusion model, and (d) Elovich model. (*continued.*).

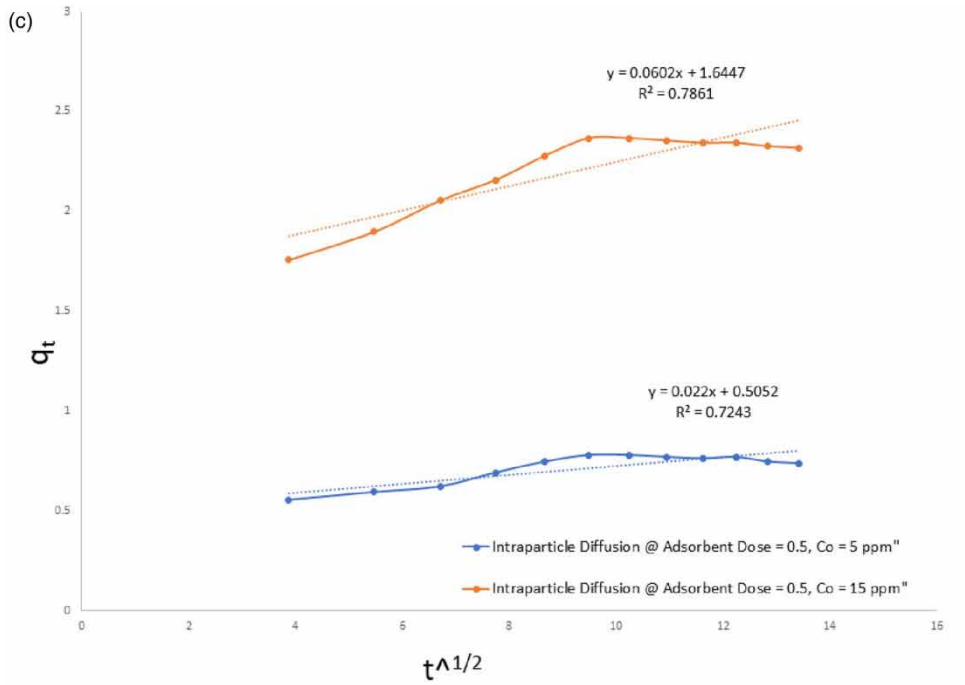

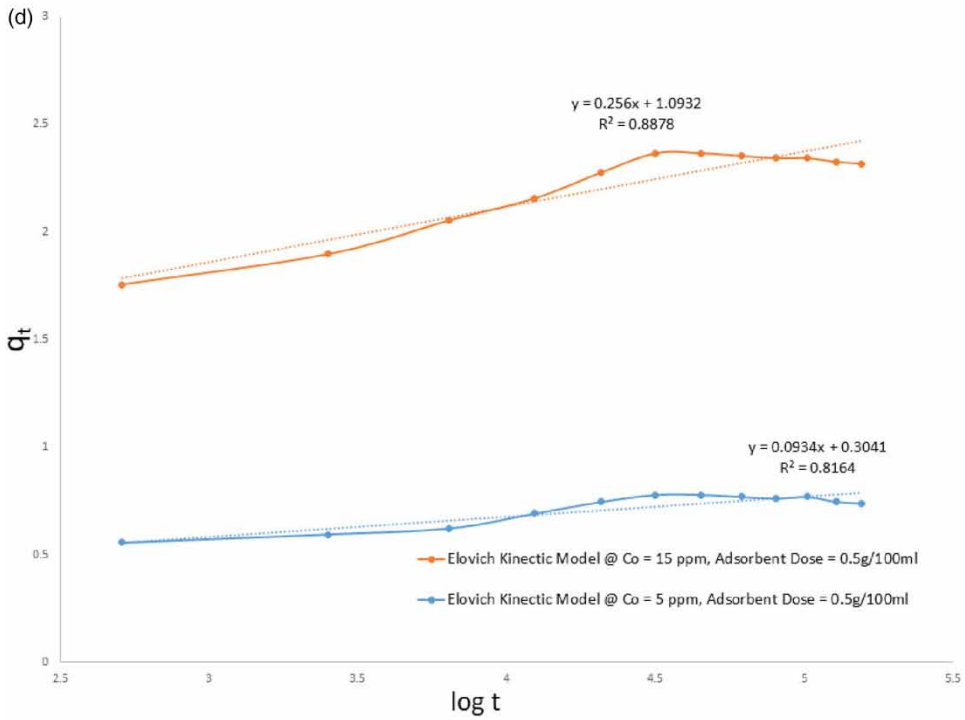

Figure 18 | Continued.

where k_{pi} denotes the rate parameter. C_i tells us about the thickness of the boundary layer. If q_t versus $t^{1/2}$ is linear then we can say intraparticle diffusion is occurring, and if it also passes through the origin, then we will be sure that the rate-limiting mechanism is only governed by intraparticle diffusion. In other cases when the graph is linear but not passing through the origin some other mechanism is also contributing to the intraparticle diffusion mechanism.

The Elovich model is needed for getting the kinetics of the adsorption process on heterogeneous surfaces, to investigate the kinetics of chemisorption, and can be expressed as:

$$q_t = \frac{1}{\beta}\ln(\alpha\beta) + \frac{1}{\beta}\ln(t) \tag{16}$$

where q_t is the amount adsorbed, α and β represents Elovich coefficients, and the linear plot of qt versus lnt will be used to get the values of Elovich coefficients. α gives us an idea about the initial sorption rate and β represents the extent of surface coverage and activation energy.

It is apparent from all the kinetics models as represented by Figure 18(a)–(d) that the adsorption capacity of STG increased rapidly for lead(II) in the first few minutes and then steadily increased until the adsorption equilibrium was achieved (i.e. 90 min). The parameters obtained from all the studied kinetic models for the removal of lead(II) onto STG was tabulated in Table 6. A correlation coefficient value >0.99 was found when we evaluated pseudo-second-order kinetics. After evaluation of all the parameters from all four kinetics models studied, it can be concluded that the experimental data is best represented by the pseudo-second-order model compared to the other kinetic model for lead(II) adsorption onto STG.

Comparison of the adsorption capabilities

The lead(II) adsorption capacity of STG was compared with other biosorbents found in the literature. The values are given in Table 7. From the table, STG was found as an efficient adsorbent with good metal scavenging capabilities.

Desorption study

For maintaining the biosorption process to be cost effective as an alternative to other wastewater treatment schemes, the regeneration or recyclability of biosorbent is very important. In this experiment, 1 g/l of the STG was used for lead(II) adsorption. The initial metal ion concentration of lead(II) ion was taken as 50 mg/l at optimum pH and stirring speed. The duration of sorption taken was for 6 h. The adsorbent was regenerated using 0.1 M HNO_3, and then washed with double distilled water. After drying it is used in subsequent cycles. In the first cycle, the removal efficiency and adsorption capacity come at 87.37% and 19.66 mg/g,, respectively, which decreased to 78.43% and 17.648 mg/g, respectively. After the third cycle it again decreased slightly 71.63% and 16.118 mg/g. The sorption of the lead(II) ions from STG declined in the next cycles also. It was observed that regenerated STG using 0.1 M HNO_3 can be used for up to three cycles without losing much of its metal scavenging capabilities. This desorption study result might be due to a decrease in available active sites after 2–3 cycles of regeneration because they were inactivated in the first cycle. Thus, diffusion of the metal ions into the inner structure of the prepared adsorbent; therefore, the extractant has a weaker ability to recover such occupied sites.

Table 6 | Kinetic model parameters of lead(II) adsorption on STG

Model	Parameters	Values
Pseudo-first-order kinetics	Q_e (mg/g)	2.4668
	k_1 (min^{-1})	0.023
	R^2	0.6256
Pseudo-second-order kinetics	k_2 (g mg^{-1} min^{-1})	0.068
	Q_e (mg/g)	2.43
	R^2	0.9984
Intraparticle diffusion model	K_{int} (mg g^{-1} s^2)	0.059
	C	1.654
	R^2	0.7762
Elovich model	α	3.9447
	β	19.6545
	R^2	0.8826

Table 7 | Comparison of adsorption capacities (mg/g) of different biosorbents for the removal of metal ions reported in the literature works

Adsorbents	Adsorption capacity (mg/g)	References
Pea nut husk	29.41	Li *et al.* (2007)
Orange peels	1.22	Xuan *et al.* (2006)
Tree leaves	21	Baig *et al.* (1999)
Rice husk	11	Chuah *et al.* (2005)
Saw dust	3	Shukla & Pai (2005)
Poplar leaves and branches	1.71	Amin (2010)
Coca shells	33	Meunier *et al.* (2003)
Tree barks	21	Martin-Dupont *et al.* (2002)
Areca waste	3.57	Li *et al.* (2010)
STG	24.272	This study

CONCLUSION

Discharged heavy metals with wastewater cause many environmental and health effects. The solution would be preventing the discharge of heavy metal directly into the water bodies. Adsorption is one of the important processes for the removal of heavy metals from wastewater. STGs are a cheap and available material discarded as waste material from tea stalls to hotels in the environment without any treatment and can be converted into adsorbent for lead(II) removal from an aqueous solution.

RSM analysis indicates that STG is a potential adsorbent with a desirability function of 0.619. Desirability analysis provided the inference about the optimum response regarding the adsorption capacity of STG as 8.9087 mg/g when process variables were 38.75 mg/l (initial concentration), 5.20655 (pH), stirring speed of 119.32, and 3.25 g/l (STG dose) for a contact time of 135.05 min at a desirability value of 0.619.

STG characterization shows a high surface area for the adsorption. The STG was determined as a potential effective adsorbent in the removal of lead(II) from aqueous solutions. The optimum adsorption at which lead(II) ions uptake is maximum was at around pH 5. The rate of adsorption was found to be quite rapid during the initial contact.. Equilibrium is achieved within 90 min for adsorbing a significant amount of lead(II) ions onto STG. Four isotherm models were used for the analysis of experimental data (i.e. Langmuir, Freundlich, Temkin, D–R isotherm models). The adsorption process is showing monolayer formation and can be easily explained by the Langmuir isotherm having an adsorption capacity of 24.272 mg/g. By kinetics studies evaluation we can conclude that the pseudo-second-order kinetics model for lead(II) ions adsorption onto STG was the most suitable kinetic model.

The highest removal efficiency was found using kinetics models. It is found to be 94.33% when under optimum conditions for $C_o = 5$ ppm we use an adsorbent dose of 0.5 g/100 ml. The adsorption mechanism and its uptake capacity were dependent on various parameters such as the pH of the aqueous solution, STG dose, initial metal ion concentration, contact time, stirring speed and particle size. The results of this study showed that STG could be suitably used as an alternative and effective adsorbent material for the removal of lead(II) ions from aqueous solutions. Based on the present study, STG can be considered as a low cost, locally and freely abundantly available, eco-friendly, and efficient bio-adsorbent for removal of lead(II) from aqueous solutions. After detailed experimental investigation we can say that RSM modelling gives us a good indication of potential adsorbents, but developing an adsorbent which can be scaled-up requires detailed experimental investigation.

DATA AVAILABILITY STATEMENT

All relevant data are included in the paper or its Supplementary Information.

CONFLICT OF INTEREST

The authors declare there is no conflict.

REFERENCES

Ahluwalia, S. S. & Goyal, D. 2005 Removal of heavy metals by waste tea leaves from aqueous solution. *Engineering in Life Sciences* **5** (2), 158–162. https://doi.org/10.1002/elsc.200420066.

Amin, Y. 2010 Biosorption of cadmium, lead, and uranium by powder of poplar leaves and branches. 976–987. https://doi.org/10.1007/s12010-009-8568-1.

Ang, S. Y., Najwa, N. F., Halim, H. N. A., Rozi, S. K. M., Mokhtar, Z., Tan, L. S. & Jusoh, N. W. C. 2022 Potential of fatty acid-modified spent tea leaves as adsorbent for oil adsorption. *Progress in Energy and Environment* **17** (1), 32–41. https://doi.org/10.37934/progee.17.1.3241.

Babel, S. & Kurniawan, T. A. 2003 Low-cost adsorbents for heavy metals uptake from contaminated water: a review. *Journal of Hazardous Materials* **97** (1–3), 219–243. https://doi.org/10.1016/S0304-3894(02)00263-7.

Baig, T. H., Garcia, A. E., Tiemann, K. J. & Paso, E. 1999 Adsorption of heavy metal ions by the biomass of solanum Elaeagnifolium (Silverleaf Night- Shade). In *Hazardous Waste Research Conference Proceedings*, January 1999, pp. 131–142.

Bailey, S. E., Olin, T. J., Mark Bricka, R. & Dean Adrian, D. 1999 *and 2 USAE Waterways Experiment Station*, *3909 Halls Ferry Rd*. *33*(11).

Chuah, T. G., Jumasiah, A., Azni, I., Katayon, S. & Thomas Choong, S. Y. 2005 Rice husk as a potentially low-cost biosorbent for heavy metal and dye removal: an overview. *Desalination* **175** (3), 305–316. https://doi.org/10.1016/j.desal.2004.10.014.

Demirbas, A. 2008 Heavy metal adsorption onto agro-based waste materials: a review. *Journal of Hazardous Materials* **157** (2–3), 220–229. https://doi.org/10.1016/j.jhazmat.2008.01.024.

Gholamiyan, S., Hamzehloo, M. & Farrokhnia, A. 2020 RSM optimized adsorptive removal of erythromycin using magnetic activated carbon: adsorption isotherm, kinetic modeling and thermodynamic studies. *Sustainable Chemistry and Pharmacy* **17** (May), 100309. https://doi.org/10.1016/j.scp.2020.100309.

Guclu, C., Alper, K., Erdem, M., Tekin, K. & Karagoz, S. 2021 Activated carbons from co-carbonization of waste truck tires and spent tea leaves. *Sustainable Chemistry and Pharmacy* **21** (December 2020), 100410. https://doi.org/10.1016/j.scp.2021.100410.

Hammud, K. K., Khalaf Hammud, K., Kadham, E. M., Raouf, A. M., Neema, R. R., Mohammed, A. & Al-Sammarrie, A. 2016 FTIR, XRD, AFM, and SEM spectroscopic studies of chemically Mw-Waste cooked tea activated carbon. *Ijrpc* **6** (3), 543–555.

Hussain, S., Anjali, K. P., Hassan, S. T. & Dwivedi, P. B. 2018 Waste tea as a novel adsorbent: a review. *Applied Water Science* **8** (6), 1–16. https://doi.org/10.1007/s13201-018-0824-5.

Kavand, M., Eslami, P. & Razeh, L. 2020 The adsorption of cadmium and lead ions from the synthesis wastewater with the activated carbon: optimization of the single and binary systems. *Journal of Water Process Engineering* **34** (October 2019), 101151. https://doi.org/10.1016/j.jwpe.2020.101151.

Lavecchia, R., Pugliese, A. & Zuorro, A. 2010 Removal of lead from aqueous solutions by spent tea leaves. *Chemical Engineering Transactions* **19** (March), 73–78. https://doi.org/10.3303/CET1019013.

Li, Q., Zhai, J., Zhang, W., Wang, M. & Zhou, J. 2007 Kinetic studies of adsorption of Pb(II), Cr(III) and Cu(II) from aqueous solution by sawdust and modified peanut husk. *Journal of Hazardous Materials* **141** (1), 163–167. https://doi.org/10.1016/j.jhazmat.2006.06.109.

Li, X., Zheng, W., Wang, D., Yang, Q., Cao, J. & Yue, X. 2010 Removal of Pb (II) from aqueous solutions by adsorption onto modi fi ed areca waste : kinetic and thermodynamic studies. *DES* **258** (1–3), 148–153. https://doi.org/10.1016/j.desal.2010.03.023.

Marshall, W. E. & Champagne, E. T. 1995 Agricultural byproducts as adsorbents for metal ions in laboratory prepared solutions and in manufacturing wastewater. *Journal of Environmental Science and Health. Part A: Environmental Science and Engineering and Toxicology* **30** (2), 241–261. https://doi.org/10.1080/10934529509376198.

Martin-Dupont, F., Gloaguen, V., Granet, R., Guilloton, M., Morvan, H. & Krausz, P. 2002 Heavy metal adsorption by crude coniferous barks: a modelling study. *Journal of Environmental Science and Health – Part A Toxic/Hazardous Substances and Environmental Engineering* **37** (6), 1063–1073. https://doi.org/10.1081/ESE-120004523.

Meunier, N., Laroulandie, J., Blais, J. F. & Tyagi, R. D. 2003 Cocoa shells for heavy metal removal from acidic solutions. *Bioresource Technology* **90** (3), 255–263. https://doi.org/10.1016/S0960-8524(03)00129-9.

Mondal, M. K. 2010 Removal of Pb(II) from aqueous solution by adsorption using activated tea waste. *Korean Journal of Chemical Engineering* **27** (1), 144–151. https://doi.org/10.1007/s11814-009-0304-6.

Omar, P. J. 2015 Geomatics techniques based significance of morphometric analysis in prioritization of watershed. *Science Technology & Engineering* **4**, 13–24.

Omar, P. J., Rai, S. P. & Tiwari, H. 2022 Study of morphological changes and socio-economic impact assessment: a case study of Koshi River. *Arabian Journal of Geosciences* **15** (17), 1426. https://doi.org/10.1007/s12517-022-10723-0.

Periasamy, K. & Namasivayam, C. 1995 Removal of nickel(II) from aqueous solution and nickel plating industry wastewater using an agricultural waste: peanut hulls. *Waste Management* **15** (1), 63–68. https://doi.org/10.1016/0956-053X(94)00071-S.

Saeed, A., Iqbal, M. & Akhtar, M. W. 2005 Removal and recovery of lead(II) from single and multimetal (Cd, Cu, Ni, Zn) solutions by crop milling waste (black gram husk). *Journal of Hazardous Materials* **117** (1), 65–73. https://doi.org/10.1016/j.jhazmat.2004.09.008.

Sahu, A., Chatterjee Mitra, J. & Author, C. 2018 Preparation of thermo-modified tea waste and its use to study the heavy metal adsorption from waste water. *IOSR Journal of Applied Chemistry (IOSR-JAC* **11** (7), 40–46. https://doi.org/10.9790/5736-1107024046.

Sekar, M., Sakthi, V. & Rengaraj, S. 2004 Kinetics and equilibrium adsorption study of lead(II) onto activated carbon prepared from coconut shell. *Journal of Colloid and Interface Science* **279** (2), 307–313. https://doi.org/10.1016/j.jcis.2004.06.042.

Shanmugaprakash, M., Venkatachalam, S., Rajendran, K. & Pugazhendhi, A. 2018 Biosorptive removal of Zn(II) ions by Pongamia oil cake (Pongamia pinnata) in batch and fixed-bed column studies using response surface methodology and artificial neural network. *Journal of Environmental Management* **227** (September), 216–228. https://doi.org/10.1016/j.jenvman.2018.08.088.

Shekhar, S., Chauhan, M. S., Omar, P. J., Jha, M., 2021 River discharge study in river ganga, varanasi using conventional and modern techniques. In: *The Ganga River Basin: A Hydrometeorological Approach* (Chauhan, M. S. & Ojha, C. S. P., eds). Springer International Publishing, pp. 101–113. https://doi.org/10.1007/978-3-030-60869-9_7

Shukla, S. R. & Pai, R. S. 2005 Adsorption of Cu(II), Ni(II) and Zn(II) on dye loaded groundnut shells and sawdust. *Separation and Purification Technology* **43** (1), 1–8. https://doi.org/10.1016/j.seppur.2004.09.003.

Simón, D., Palet, C., Costas, A. & Cristóbal, A. 2022 Agro-Industrial waste as potential heavy metal adsorbents and subsequent safe disposal of spent adsorbents. *Water (Switzerland)* **14** (20). https://doi.org/10.3390/w14203298

Singh, S. R. & Singh, A. P. 2012 Adsorption of heavy metals from waste waters. *Global Journal of Researches in Engineering* **12** (1), 3–7.

Sujatha, S. & Sivarethinamohan, R. 2021 Application of response surface methodology to optimize lead(Ii) ion adsorption by activated carbon fabricated from de oiled soya. *Desalination and Water Treatment* **226**, 242–250. https://doi.org/10.5004/dwt.2021.27240.

Xuan, Z., Tang, Y., Li, X., Liu, Y. & Luo, F. 2006 Study on the equilibrium, kinetics and isotherm of biosorption of lead ions onto pretreated chemically modified orange peel. **31**, 160–164. https://doi.org/10.1016/j.bej.2006.07.001.

Yoshita, A., Lu, J. L., Ye, J. H. & Liang, Y. R. 2009 Sorption of lead from aqueous solutions by spent tea leaf. *African Journal of Biotechnology* **8** (10), 2212–2217. https://doi.org/10.5897/AJB2009.000-9287.

Zuorro, A. & Lavecchia, R. 2010 Adsorption of Pb(II) on spent leaves of green and black tea. *American Journal of Applied Sciences* **7** (2), 153–159. https://doi.org/10.3844/ajassp.2010.153.159.

First received 31 January 2023; accepted in revised form 27 April 2023. Available online 11 May 2023